Estimation of NO_x and SO_2 Emissions from Sarnia, Ontario using Mobile-MAX-DOAS and a NO_x-Analyzer

Zoe Y. W. Davis[1], Sabour Baray[2], Chris A. McLinden[3], Aida Khanbabakhani[2], William Fujs[2], Csilla Csukat[2], Jerzy Debosz[4], Robert McLaren[2].

[1]Graduate Program in Earth and Space Science, York University, Toronto, M3J 1P3, Canada
[2]Centre for Atmospheric Chemistry, York University, Toronto, M3J 1P3, Canada
[3]Environnment and Climate Change Canada, Toronto, M3H 5T4, Canada
[4]Air Quality Monitoring and Assessment Unit, Ontario Ministry of the Environment, Conservation and Parks, Etobicoke, M9P 3V6, Canada

Correspondence to: Zoe Y. W. Davis (zoeywd@yorku.ca) or R. McLaren (rmclaren@yorku.ca)

Abstract. Sarnia, ON experiences pollutant emissions disproportionate to its relatively small size. The small size of the city limits traditional top-down emission estimate techniques (e.g., satellite) but a low-cost solution for emission monitoring is Mobile-MAX-DOAS. Measurements were made using this technique from 21/03/2017 to 23/03/2017 along various driving routes to retrieve vertical column densities (VCDs) of NO_2 and SO_2 and to estimate emissions of NO_x and SO_2 from the Sarnia region. A novel aspect of the current study was the installation of a NO_x analyzer in the vehicle to allow real time measurement and characterization of near-surface NO_x/NO_2 ratios across the urban plumes, allowing improved accuracy of NO_x emission estimates. Confidence in the use of near-surface measured NO_x/NO_2 ratios for estimation of NO_x emissions was increased by relatively well-mixed boundary layer conditions. These conditions were indicated by similar temporal trends in NO_2 VCDs and mixing ratios when measurements were sufficiently distant from the sources. Leighton ratios within transported plumes indicated peroxy radicals were likely disturbing the $NO\text{-}NO_2\text{-}O_3$ photostationary state through VOC oxidation. The average lower limit emission estimate of NO_x from Sarnia was 1.60 ± 0.34 tonnes hr^{-1} using local 10 m elevation wind-speed measurements. Our estimates were larger than the downscaled annual 2017 NPRI reported industrial emissions of 0.9 tonnes NO_x hr^{-1}. Our lower limit estimate of SO_2 emissions from Sarnia was 1.81 ± 0.83 tonnes SO_2 hr^{-1}, equal within uncertainty to the 2017 NPRI downscaled value of 1.85 tonnes SO_2 hr^{-1}. Satellite-derived NO_2 VCDs over Sarnia from the Ozone Monitoring Instrument (OMI) were lower than Mobile-MAX-DOAS VCDs, likely due to the large pixel size relative to the city's size. The results of this study support the utility of the Mobile-MAX-DOAS method for

estimating NO_x and SO_2 emissions in relatively small, highly industrialized regions especially when supplemented with mobile NO_x measurements.

1 Introduction

Differential Optical Absorption Spectroscopy (DOAS) is a remote sensing technique that quantifies tropospheric trace-gases using light spectra and the unique spectral absorption cross sections of trace-gases. DOAS has been used since its introduction by (Platt et al., 1979) to measure small molecular species including NO_2, SO_2, OH, BrO, NO_3, NH_3, ClO and others. One advantage of the technique is the potential for simultaneous quantification of multiple trace-gases (e.g., SO_2 and NO_2) (Platt et al., 2008). The Multi-Axis DOAS (MAX-DOAS) method allows sensitive quantification of tropospheric pollutants by measuring scattered sunlight spectra at multiple viewing directions and/or elevation angles. Spectra measured at elevation angles close to horizon-pointing have high sensitivity to ground-level gases since the light paths are longer near the surface (Honninger et al., 2004). Ground-based MAX-DOAS measurements quantify total boundary layer pollution loading by determining tropospheric vertical column densities (VCDs) of trace-gases. These measurements are, therefore, well suited to measureing total emissions into an air mass. VCDs are independent of boundary layer height, unlike mixing ratios, and are spatially averaged (horizontally and vertically) on the order of a few kilometres along the light path. Ground-based MAX-DOAS can also retrieve vertical profiles of aerosol extinction and trace-gases by combining MAX-DOAS data with radiative transfer modelling (Friess et al., 2006; Heckel et al., 2005; Honninger et al., 2004; Honninger and Platt, 2002; Irie et al., 2008; Wagner et al., 2004, 2011).

The recently developed Mobile-MAX-DOAS technique allows measurement of trace-gas emissions from a region of interest by driving the instrument around the region. The method can estimate emissions on a nearly hourly basis in a region with a spatial resolution of ~1 km. Mobile MAX-DOAS has been used to estimate NO_x emissions from a shipping and industrial areas (Rivera et al., 2010), power-plants (Wu et al., 2017) and cities (Ibrahim et al., 2010; Shaiganfar et al., 2011, 2017), validate satellite and air quality modelled VCDs (Dragomir et al., 2015; Shaiganfar et al., 2015), estimate surface NO_2 mixing ratios from NO_2 VCDs (Shaiganfar et al., 2011), and determine the horizontal variability of trace-gas VCDs within satellite pixels (Wagner et al., 2010). Mobile-MAX-DOAS is a "top-down" approach for quantifying real-world emissions that can be used to validate "bottom-up" emission inventories (Shaiganfar et al., 2011).

Sarnia, Ontario, a small Canadian city, experiences pollutant emissions due to a large number of industrial chemical and oil processing facilities, vehicular exhaust from the Canada-U.S.A. international border crossing, emissions from large ships travelling through the St Clair River, vehicular traffic, residential heating and other anthropogenic emissions from the city populace, and transnational air pollution from Ohio, Illinois and Michigan (Oiamo et al., 2011). These sources contribute to increased levels of air pollutants such as NO_x, VOC's and SO_2, which are precursors of $PM_{2.5}$ and O_3 (Ministry of the Environment and Climate Change, 2015). Traditional "top-down" methods for quantifying pollutant emissions from small cities (e.g., satellite monitoring, aircraft studies) are limited by the small footprint. Additionally, in-situ air quality monitoring stations are limited by the bias towards near-surface emissions and under-sampling of elevated emissions (Tokarek et al., 2018).

The Mobile-MAX-DOAS method has advantages over satellite, aircraft and in-situ techniques. Major advantages over satellite techniques include 1) emissions can be estimated without the need for an a-priori vertical profile, 2) accuracy of estimates can increase rather than decrease for smaller source regions, and 3) emissions may be estimated many times per day. Satellite retrievals are useful for estimating "top-down" emissions on regional and global scales over long periods of time (Huang et al., 2014; Kim et al., 2014; Liu et al., 2016; McLinden et al., 2012). However, accuracy over small regions can be limited by insufficient pixel resolution due to horizontal averaging and retrieval reliance on modelled a-priori vertical profiles that may not resolve small regions (Heckel et al., 2011). Aircraft studies can quantify emissions from cities but are relatively expensive. The major advantage of emissions estimates using aircraft measurements is that one can in principle fully characterize the vertical profile of trace gas concentration as well as the vertical profile of wind vectors for an accurate horizontal flux measurement downwind of a source (Baray et al., 2018; Gordon et al., 2015). Major advantages of the Mobile-MAX-DOAS method over aircraft techniques are that 1) MAX-DOAS VCDs are already vertically integrated, reducing the uncertainties due to interpolation of measurements at multiple flight altitudes and 2) MAX-DOAS studies are logistically easier to conduct. However one is still left with the uncertainty of the vertical profile of wind vector fields. The Mobile-MAX-DOAS technique is a solution for quantifying pollutant emissions that complements the aforementioned techniques as well as in-situ monitoring, through the ability to observe localized surface based and elevated emissions.

An uncertainty associated with MAX-DOAS and satellite methods when estimating NO_x emissions from NO_2 measurements is the assumptions concerning the NO_x/NO_2 relationship in the air mass, which can be variable both spatially and temporally. The NO_x/NO_2 ratio is often assumed to be spatially constant, taken from literature based on the season,estimated using atmospheric modelling or occasionally taken from aircraft measurements when available (Rivera et al., 2010). In this study, we combined the Mobile-MAX-DOAS method with simultaneous mobile NO_x measurements (NO, NO_2, NO_x) to increase knowledge of the NO_x/NO_2 ratio in the air mass spatially and temporally in order to improve the accuracy of the NO_x emission estimates obtained from NO_2 measurements. A stationary modular meteorological station was deployed in the airshed provided auxillary meteorological information, typically a major source of uncertainty in Mobile-MAX-DOAS emission estimations. Hourly wind data measured at 10 m elevation (agl) were also available from local, permanent monitoring stations. Vertical wind profiles were modelled in high resolution (1 km x 1 km) using the version 3.9.1 Weather Research and Forecasting model (WRF) centred on Sarnia (42.9745^o N, 82.4066^o W) in an attempt to improve upon emissions values calculated using near-surface wind-speed, since wind-speeds are expected to increase with altitude. However, inter-comparison of WRF modelled winds with measured near-surface winds during the study period indicated poor model performance (see Supplement S2.2 for detailed results). Emissions in this study were therefore calculated using the 10 m measured winds to provide lower limit estimates of the hourly emissions.

Our study objectives were to 1) examine the relationship between the NO_2 near-ground mixing ratios and the NO_2 tropospheric VCDs, 2) determine NO_x and SO_2 emissions from the city of Sarnia including industrial sources, 3) determine the impact of NO_x/NO_2 variability on the accuracy of NO_x emission estimates, and 4) examine OMI satellite intrapixel NO_2 homogeneity. This study aims to demonstrate the utility of this method for determining trace-gas emissions and monitoring pollutant transportation in Sarnia and similar urban/industrial areas.

2 Experimental

2.1 Location and Instruments

Measurements were conducted in and around the city of Sarnia (42.9745° N, 82.4066° W), located in southwestern Ontario, Canada at the border with Port Huron, MI, U.S.A (Fig.1). The routes driven in the vehicle aimed to capture major NO_x and SO_2 emission sources at different distances downwind, dependent on the prevailing wind conditions.

The metro area has a population of ~72,000 (2016 census) and an area of ~165 km^2. Sources of air pollution in this region include emissions from large ships, anthropogenic emissions from the cities of Sarnia and Port Huron, transport from the cities of Windsor and Detroit (60 km SW), the St Clair and Belle River power-plants (20 km SSW), oil refineries and chemical industry in Sarnia, and the cross-border traffic between Canada and the U.S.A. along Highway 402. Emissions from ships along the St. Clair River, normally a major source, were absent during the time of our study since the canal had not opened for the season.

A mini-MAX-DOAS instrument (Hoffmann Messtechnik GmbH) measured scattered sunlight spectra during three days: 21/03/2017 to 23/03/2017 ("Days 1 to 3") while mounted on top of a car in a backwards pointing direction. The instrument has a sealed metal box containing entrance optics, UV fibre coupled spectrometer and electronics. Incident light is focused on a cylindrical quartz lens (focal length = 40 mm) into a quartz fibre optic that transmits light into the spectrometer (OceanOptics USB2000) with a field of view approximately 0.6^o. The spectrometer has a spectral range of 290-433 nm, a 50µm wide entrance slit yielding a spectral resolution was ~0.6 nm. The spectrometer is cooled and stabilized by a Peltier cooler. Spectrometer data was transferred to a laptop computer via USB cable. Spectra were obtained with an integration time of ~1 minute with the continuously repeating sequence of viewing elevation angles (30^o, 30^o, 30^o, 30^o, 40^o, 90^o). The vehicle was driven at a low but safe target speed of 50 km hr^{-1} when possible to provide a spatial resolution of ~ 1 km, but speeds were occasionally up to 80 km hr^{-1} when necessary. Tropospheric VCDs were estimated from the 30^o and 40^o elevation angle spectra. The 40^o spectra allow verification that aerosol levels were sufficiently low to determine VCDs without radiative transfer modelling since VCDs obtained from both angles should be equal within ±15% under low to moderate aerosol loading conditions (Wagner et al., 2010). The cool temperatures in March aided in this as secondary organic aerosol loading tends to be low in this season due to an absence of biogenic emissions.

A Model 42 chemiluminescence NO-NO_2-NO_x Analyzer (Thermo Environmental Instruments Inc.) mounted in the vehicle measured NO, NO_2, and NO_x ($NO+NO_2$) near-surface mixing ratios. A PTFE inlet tube (5m length and ID=1/4") was mounted above the front vehicle window on the passenger side (~1.5 m above ground). The instrument alternately recorded average NO-NO_2-NO_x mixing ratios with a temporal resolution of 1 minute. Most of the routes were driven downwind of Sarnia on rural remote roads with little to no traffic such that NO_x emissions from other vehicles were not a concern. When NO_x from other vehicles was a potential concern, data was filtered

out via careful note taking. The instrument indirectly measures NO_2 by subtracting the NO chemiluminescence signal obtained when air bypasses a heated Molybdenum (Mo) convertor from the successive total NO_x chemiluminescence signal obtained when air passes over the Mo-convertor. The NO_x analyzer can overestimate NO_x and NO_2 due to the potential contribution of other non-NO_x reactive nitrogen oxides (NO_z) other than NO_2 that can also be reduced to NO by the Mo converter (HNO_3, HONO, organic nitrates, etc.), leading to an overestimation (Dunlea et al., 2007). Since this overestimation is more important in low NO_x regions, only data with NO_x mixing ratios > 3 ppb were used. Mixing ratios of <3ppb NO_2 were only measured outside of plume-impacted regions when NO_2 VCDs were also low. The potential error in NO_x/NO_2 ratios is addressed further in section 3.2. NO_x mixing ratios can also have an error when successive NO and NO_x measurements occurred in areas with a significant temporal gradient in the NO_x emissions. Such gradients were seen due to passing vehicles or localized industrial NO_x plumes. These data were removed based on records of passing vehicles and other local near-surface sources or whenever the NO_2 mixing ratios were reported as negative. Few data points were removed because the routes driven were primarily rural roads with extremely low traffic density.

Aura satellite Ozone Monitoring Instrument (OMI) data were obtained for overpasses of the Sarnia, Ontario area for Days 1 and 3. Tropospheric NO_2 VCDs are the NASA Standard Product Version 3.0 with AMFs recalculated using the Environment and Climate Change Canada regional air quality forecast model GEM-MACH. The OMI instrument makes UV-vis solar backscatter radiation measurements with a spatial resolution of 13x24 km^2 at nadir and up to 28×150 km^2 at swath edges (Ialongo et al., 2014). The NO_2 detection limit of OMI is 5×10^{14} molec cm^{-2} (Ialongo et al., 2016). The OMI data used were screened for row anomalies that have affected OMI data since June 2007 (Boersma et al., 2007).

2.2 MAX-DOAS Determination of VCDs

Trace-gas Differential Slant Column Densities (DSCDs) were obtained using the DOAS technique (Platt et al., 2008) with the spectral fitting range of 410-435 nm for NO_2 at 293 K and 307.5-318 nm for SO_2 at 293 K. All trace-gas cross-sections used were from (Bogumil et al., 2003). For both gases, spectral fits also included a Fraunhofer Reference Spectrum (FRS), Ring Spectrum created from the FRS, O_3 cross-sections at 223 K and 297 K, and a third-order polynomial. The NO_2 cross-section was included in the SO_2 fits. Formaldehyde (HCHO) was not included in the fits for SO_2 as it was expected to be very low, and did not affect the residuals for the SO_2 fits. NO_2

DSCDs from Day 1 were fit against a single, same-day FRS obtained in a low-pollutant region near solar-noon time. These DSCDs were corrected for SCD(FRS) and SCD(Solar Zenith Angle (SZA)) contributions using the $DSCD_{offset}$ method (Wagner et al., 2010). The SCD(FRS) is the constant tropospheric trace-gas SCD component present in the FRS that causes an underestimation in the fitted DSCD. The SCD(SZA) is the difference between the stratospheric trace-gas component in the FRS and the measured non-zenith spectra. SCD(SZA) varies over time of day (t_i), maximizing overestimation in the DSCD early and late in the day. The sum of SCD(FRS) and SCD(SZA) is collectively known as the $DSCD_{offset}$. The $DSCD_{offset}(t_i)$ function was estimated by fitting a second order polynomial to multiple pairs of DSCDs of spectra (non-zenith and zenith from the same sequence), described in detail in (Wagner et al., 2010).

The $DSCD_{offset}$ polynomial is most accurate when successive spectra in each sequence observe similar mixing ratio fields, and measurements obtained many data-points over most of the daylight hours. However, routes on Days 2 and 3 included driving in and out of both high and low NO_x regions within short time-periods and thus met neither of the requirements listed above for the $DSCD_{offset}$ method. On these days, a second method was used where NO_2 DSCDs were fit against an FRS spectrum obtained close in time (<25 minutes) along each respective route in a low-pollutant region. The impacts of SCD(FRS) and SCD(SZA) on the retrieved DSCDs can be assumed to be negligible since each FRS was from a low-pollutant area and obtained close in time, respectively. This method was also used for the Day 1 SO_2 route since limited data were available but included background SO_2 measurements close in time.

For all routes trace-gas tropospheric VCDs were determined by assuming a single scattering event occurred for each photon such that the air-mass factor (AMF) depended only on the viewing elevation angle, $\propto$, $AMF_{trop}(\propto) \approx \frac{1}{\sin(\alpha)}$ (Brinksma et al., 2008)(Wagner et al., 2010). This "geometric approximation" is most valid under low to moderate aerosol loading and has been shown to deviate from the typically more accurate radiative transfer modelling by up to ±20% under moderate aerosol loading (Shaiganfar et al., 2011). Day 1 VCDs were calculated following Eq. (1):

$$VCD_{trop} = \frac{DSCD_{meas}(\propto, t_i) + DSCD_{offset}(t_i)}{\frac{1}{\sin(\alpha, t_i)}} \quad (1)$$

Days 2 and 3 NO_x and Day 1 SO_2 VCDs were calculated following Eq. (2):

$$VCD_{trop} \approx \frac{DSCD_{meas}(\propto, t_i)}{\frac{1}{\sin(\alpha, t_i)}} \quad (2)$$

The VCD of SO_2 was above detection limit on only two occasions in this study (both on Day 1), in contrast to NO_2. The detection limit of SO_2 is higher than NO_2 for several reasons, first, it's differential cross section is less than that of NO_2 and, second, its absorption features are in the UV wavelength region where scattered sunlight intensity is much less than that in the visible region. The fast measurements required in mobile DOAS also allow limited averaging of spectra compared to stationary measurements (Davis et al., 2019), where detection of industrial SO_2 plumes is easier. Therefore, SO_2 DSCDs were only above detection limits for Day 1 Routes 3 & 4 when the light levels were highest, and the vehicle observed the combined plumes of the largest SO_2 sources in the area.

2.3 Estimating Trace-gas Emissions from MAX-DOAS VCDs

Trace-gas emission estimates were calculated following a flux integral approximation Eq. (3):

$$E = \left[\left(\sum_i \left(VCD_{outflow,i} - VCD_{influx,i} \right) w_i \sin(\beta_i)\, ds \right] \frac{MW}{Av} \right. \quad (3)$$

where $VCD_{outflow,i}$ is the VCD measured at position i along the route s for distance ds, $VCD_{influx,i}$ is either the measured influx values or the estimated background VCD value, w_i is the wind-speed, β_i is the angle between the driving direction and the wind-direction, MW is the molecular weight of the target gas, and Av is Avogadro's number. Transect routes were designed to observe both within and beyond emission impacted areas since routes encircling the emission sources were often not possible. Flux integrals were calculated using portions of the transects impacted only by the Sarnia urban/industrial plume in cases where plumes from other sources impacted the transect (i.e., Day 1; U.S.A. power-plant plumes). In these cases, the end-points of integration were chosen judiciously where NO_2 VCDs and surface mixing ratios decreased to a minimum at the edge of the Sarnia emissions. This method assumes that the wind-field and trace-gas emission rates are constant during the time required to drive a route. The validity of this assumption improves with decreased time for driving route completion. The Sarnia region is ideal for this method since a small geographical area contains the majority of the emissions and is surrounded on three sides by rural regions with low anthropogenic emissions.

A potential source of uncertainty in Mobile-MAX-DOAS emission estimates is variation in the wind fields and/or source emission rates while driving (Ibrahim et al., 2010; Wu et al., 2017). Previous studies have estimated wind-fields from local meteorology stations (Ibrahim et al., 2010), meteorological models (Shabbir et al., 2016; Shaiganfar et al., 2011, 2017) or LIDAR measurements (Wu et al., 2017). In our study, wind field information was

obtained from a Modular Weather Station (Nova Lynx 110-WS-25DL-N) we deployed near one of the driving routes at (42.8148^{o}, -82.2381^{o}) (Fig. 1) and from meteorological ground stations in the area (Fig. 1, Table S1, Fig. S1). The modular weather station measured wind-speed and direction, temperature, relative humidity, and barometric pressure at 2 m above the surface every 30 seconds. Wind data was available from the Sarnia-Lambton Environmental Association (SLEA) LaSalle Road (42.911330°, -82.379900°) and Moore Line (42.83954°, -82.4208°) meteorological stations that are located near the driving routes (Fig. 1). These stations were surrounded by fallow, flat farm-land for at least 4 km on each side and thus should reflect total boundary layer for plumes transported away from the city more than the urban stations (Fig. S1). The hourly wind-direction data from the modular and permanent stations exhibited similar values (±10^{o}) and trends on Day 1 (Fig. S2). Wind-directions for Days 2 and 3 were obtained by determining the angle of a vector drawn between the geographical locations of the maximum NO_2 VCD enhancements and the industrial facilities expected to have emitted the plumes. These map-determined wind-directions were consistent (+/-10^{o}) with the data from the station(s) closest to the driving route. Comparison of wind-speed data on Days 2 and 3 was not possible due to a technical issue with the modular weather station on these days.

The NO_2 VCD influx (background VCD) was estimated on Day 1 since measurement was impossible along the western border of Sarnia due to the road configuration and proximity of industrial emissions. A NO_2 VCD_{influx} = 2×10^{15} molec cm^{-2} was estimated based on OMI satellite VCDs of ~1.5-3.5$\times10^{15}$ molec cm^{-2} from the area east of Sarnia that are expected to be similar to the NO_2 regime west of Sarnia. These pixels are expected to be unaffected by other sources. The influx would be expected to be impacted by vehicular and residential emissions from the small city of Port Huron, U.S.A., on the west side of the St Clair River (Fig. 1), which has limited industry but a moderate level of commercial vehicle activity due to border-crossings. A first order emission estimate of vehicular NO_x emissions from Port Huron from daily reported traffic counts results in an upper limit of NO_2 influx VCD of ~1×10^{15} molec cm^{-2} (see Supplement S4). True influx would vary along the length of the measurement transect, depending on what sources are upwind of the location. Halla et al. (2011) measured NO_2 tropospheric VCDs using MAX-DOAS in a similar region approximately 70 km south-east of Sarnia. The observed NO_2 VCDs in that study ranged from 0.01 to 1.25×10^{16} molec cm^{-2} with a median value of 2×10^{15} molec cm^{-2}, which is expected to be representative of background NO_2 columns in this region. The highest VCD in that study was attributed to the transport of industrial emissions from the Sarnia area and/or from Detroit, MI to the northwest and west of the site

239 respectively (Halla et al., 2011). Based on the range of VCDs from literature, vehicular emission estimates and
240 satellite measurements, a background VCD of 2×10^{15} molec cm^{-2} is a reasonable estimate, and emissions sensitivity
241 tests were conducted using influx VCDs of $0.5\text{-}3\times10^{15}$ molec cm^{-2} (Supplement S5). In contrast, the NO_2 VCD_{influx}
242 on Days 2 and 3 and SO_2 VCD_{influx} on Day 1 were determined from the average VCDs measured in the low-
243 pollution area of each transect.

244 **2.3.1 Determination of NO_x emission estimates from NO_2 measurements**

245 NO_x emissions were estimated using Equation 4 from the NO_2 flux integral and the average NO_x/NO_2 ratio (NO_x > 3
246 ppb) measured by the NO_x-analyzer along the route. The emission values were then corrected for expected NO_x loss
247 during transport using a NO_x lifetime, τ. NO_x emission estimates were calculated as follows:

$$\boldsymbol{E_{NOx} = E_{NO_2} * \frac{\overline{NO_x}}{NO_2} * e^{\left(\frac{y/w}{\tau}\right)}} \quad (4)$$

248 where τ is NO_x lifetime, w is wind-speed, and y is the distance between the NO_x source and the measurement
249 location. For routes where individual NO_x/NO_2 ratios deviated significantly from the route average, the NO_x
250 emission estimates were calculated by applying 1) the route-averaged NO_x/NO_2 ratio and 2) individual NO_x/NO_2
251 ratios associated with each NO_2 VCD point by point. Multiple factors determine NO_x lifetime in a plume. A NO_x
252 lifetime of 6 hours was used in this study based on considerations given in section 3.3. A sensitivity analysis was
253 performed varying the lifetimes between 4-8 hours (Supplement S7). The conversion factors used to calculate NO_x
254 emissions for each route can be found in Table S8. The NO_x/NO_2 ratios are more fully addressed in Section 3.2 and
255 the NO_x lifetime is addressed in Section 3.3.

256 **3 Results & Discussion**

257 **3.1 Relationship between NO_2 VCDs & NO-NO_2-NO_x Analyzer Measurements**

258 Figure 2 shows that enhancements in NO_2 VCDs downwind of Sarnia were generally associated with NO_2 surface
259 mixing ratios enhancements during Days 1 and 2. This suggests that pollution from Sarnia was well-mixed within
260 the boundary layer at the measurement locations, typically 14-23 km downwind of sources (Figs. 3 & 4). However,
261 the ratio of NO_2 VCD to NO_2 mixing ratio was sometimes variable even during relatively short time periods when

the boundary layer height was expected to be constant (Fig. 2a). This variability was probably due to the presence of multiple NO_x plumes that had originated from sources with different heights (i.e., stacks and surface sources) and emission rates.

In contrast to Days 1 and 2, NO_2 VCD enhancements on Day 3 were not consistently associated with NO_2 surface mixing ratio enhancements (Figs. 5 & 6). A large surface enhancement (NO_x=22 ppb) was observed at the location of the VCD NO_2 enhancements (~2.5×10^{16} molec cm^{-2}) associated with the NOVA Chemicals industrial plume on route 2 (Figs. 5b & 6b) but not on route 1 (Fig. 5a & 6a). This discrepancy is likely due to the closer proximity of the driving route to the source compared with Day 1, combined with limited vertical mixing of the plume. The relatively long sampling time of the NO_x analyzer with a relatively fast driving speed on this route may also have led to an underestimation of the true NO_x values for this localized plume.

3.2 NO_x/NO_2 Ratios

The NO_x/NO_2 ratio is necessary to estimate NO_x emissions from the source, given measurements of NO_2 VCD's (Eq. 4). Ratios of NO_x/NO_2 (Table 2) measured along the routes on Days 1 and 3 were within 20% of the route-averaged value with a relative standard deviation of less than 12%. NO_x/NO_2 ratios tended to increase at locations associated with transported plumes' centerlines, as expected due to an increase in NO emissions from the sources (see Fig. 7), and exhibited the greatest variability in air-masses affected by sources with different altitudes and emission rates. Day 1, route 1 exhibited variable NO_x/NO_2 ratios due to emissions from the power-plants across the river in Michigan, residential and vehicular traffic, and industrial emissions (Figs. 3a & 7).

Potential errors may exist in the NO_x/NO_2 ratio due to the presence of other NO_z species in the air mass (e.g., HNO_3, HONO, NO_3, N_2O_5, organic nitrates, etc.) that are also converted to NO by the Mo-convertor in addition to NO_2 (Dunlea et al., 2007). However, these errors are smaller than might be expected due to the presence of the error in both the numerator and the denominator of the ratio, $NO_x/NO_2 = (NO+NO_2)/NO_2$, thus partially offsetting each other. For example, at an apparent NO_x/NO_2 ratio of 1.40 (average in Table 2), a 10% and 30% error in the reported NO_2 due the presence of other NO_z species gives rise to errors of only -2.6% and -6.6% in the measured NO_x/NO_2 ratio respectively. Mathematically, the error in the NO_x/NO_2 ratio gets larger as the percentage of NO in the total NO_x increases. However, since most of the interfering NO_z species are generated photochemically, or only at night

(NO_3, N_2O_5) increasing with reaction time and distance away from the source, the percentage of interfering species is smaller at higher values of total NO and NO_x. Under significantly intense photochemical conditions in the MCMA-2003 field campaign in Mexico, the interference in the chemiluminescence monitors resulted in average NO_2 concentrations being 22% higher than those determined from spectroscopic measurements (Dunlea et al., 2007), which would give rise to an error in the NO_x/NO_2 ratio of <5%. In the current study we estimate that the resultant negative bias in the measured NO_x/NO_2 ratio does not exceed -5% for several reasons; i) we filter out low NO_x data (<3ppb), ii) the emission integral is dominated by regions with high NO_x that are spatially and temporally close to the sources and, iii) photochemistry was reduced during this spring campaign. The uncertainty that arises from potential errors in the NO_x/NO_2 ratio is insignificant compared to other errors (see Supplemental Table S9). It is also worth noting that NO_2 measurements by the NO_x analyzer are not directly used for the calculation of emissions; only the NO_x/NO_2 ratio is used.

Previous Mobile-MAX-DOAS studies have relied on literature estimates of the NO_x/NO_2 ratio (Shabbir et al., 2016; Shaiganfar et al., 2011) or estimated the ratio from a Leighton ratio calculated using local air quality station data (Ibrahim et al., 2010). In regions with many pollutant sources throughout (e.g., megacities), this ratio is expected to be horizontally and vertically inhomogeneous. The ratio can therefore be challenging to estimate and can increase the uncertainty of the NO_x emission estimate. Estimation of NO_x/NO_2 ratios from near-surface monitoring stations can be problematic because the ratios are applied to a VCD but may reflect only local emissions (e.g., nearby vehicular exhaust) rather than the total boundary layer. In this study, NO_x data impacted by local emissions were removed. Also, the Sarnia emissions were expected to be well mixed to the surface since most of the transects were driven sufficiently far from the sources. Therefore, the near-surface NO_x/NO_2 ratios should be representative for the altitude range of the dispersed NO_x plume(s). This hypothesis is supported by the similarity between the NO_2 surface and VCD temporal trends during the study, especially on Days 1 and 2 (Fig. 2).

3.3 NO_x Lifetime

Various lifetimes of NO_x, τ, have been used in previous mobile MAX-DOAS studies for the calculation of NO_x emissions from NO_2 measurements: 6 hr in Germany (Ibrahim et al., 2010), 5 hr in Delhi (Shaiganfar, 2011), 5 hr in China (Wu et al., 2017) and 3 hr summer – 12 hr winter in Paris (Shaiganfar, 2017). In Beirle et al. (2011), the daytime lifetime of NO_x was quantified by analyzing the downwind patterns of NO_2 measured by satellite

instruments and shown to vary from ~4 hr in low to mid-latitude locations (e.g., Riyadh, Saudia Arabia) to ~8hr in northern locations in wintertime (e.g., Moscow, Russia). In a follow up study, Valin et al (2013) showed that one cannot assume that τ is independent of wind speed and derived values of τ from the satellite observations over Riyadh to be 5.5hr to 8 hr, corresponding to OH levels of $5\text{-}8\times10^6$ molec cm^{-3}at high and low wind speeds.

Multiple factors determine NO_x lifetime in a plume, including season (e.g., insolation) (Liu et al., 2016), latitude, wind-driven dilution (Nunnermacker et al., 2000; Valin et al., 2013), NO_x emission rate and initial dilution (Nunnermacker et al., 2000), temperature, hydroxyl radical levels (OH) and precursors to OH including O_3, H_2O, and HONO. Very importantly, the daytime lifetime of NO_x is a nonlinear function of the NO_x concentration itself, having longer lifetimes at high and low concentrations with the shortest lifetimes at intermediate NO_x concentrations due to the impact on OH levels in a non-linear feedback on its own lifetime (Valin et al., 2013). The NO_x lifetime is ultimately dependent on the OH levels since this dictates the loss rate of NO_2 to its terminal sink ($NO_2 + OH \rightarrow HNO_3$). However the presence of VOC's in the urban plume, which are catalytically oxidized forming O_3 in the presence of NO_x and HO_x ($OH + HO_2$), can decrease the NO_x lifetime due to their acceleration of the conversion of NO to NO_2 via peroxy radical reactions ($RO_2^{\cdot} + NO \rightarrow NO_2 + RO^{\cdot}$). Therefore, NO_x lifetimes can vary both spatially and temporally (Liu et al., 2016), even within the same plume (Valin et al., 2013). Underestimation of the true NO_x lifetime leads to overestimation of the NO_x emissions, while an overestimate leads to an underestimation of the emissions.

While photolysis of HONO is often the major source of OH in the morning boundary layer (Platt et al., 1980; Alicke et al., 2002), midday production of OH via photolysis of O_3 and subsequent reaction of O (^1D) with water is frequently the dominant source of OH. Assuming $O(^1D)$ is in steady-state, it can be shown that when ozone photolysis is the main source of OH, the product of the mixing ratios of H_2O and O_3 is proportional to the production rate of OH. In this study, the $[H_2O]*[O_3]$ product was calculated using surrounding station measurements (see Supplement S8.1). The $[H_2O]*[O_3]$ product indicates that mid-day OH production under the spring-conditions for Days 1 and 2 is only 10-25% of the expected OH production under warmer more humid summer-conditions, presuming that O_3 photolysis predominates. This might suggest OH levels were lower in our study than during summer, and hence NO_x lifetimes longer. However we assume this with caution as the HONO production is not known nor are the loss rates of OH.

As mentioned, the presence of VOC's can decrease the lifetime of NOx under conditions where NOx is sufficiently high to dominate the peroxy radical reaction path. To test for the presence of VOC's in the plumes (in the absence of measurements), Leighton ratios, ϕ (Leighton, 1961), were calculated at locations of maximum NO_2 VCD associated with Sarnia plumes. Leighton ratios were calculated following Eq. (5) (see Supplement S8.2 for details):

$$\phi = \frac{\boldsymbol{j_{NO2}[NO_2]}}{\boldsymbol{k_8[NO][O_3]}} \quad (5)$$

where j_{NO2} is the NO_2 photolysis rate, k_8 is the temperature-dependent rate constant for the reaction between NO and O_3. Leighton ratios equal to 1.0 indicate that NO, NO_2 and O_3 are in steady state with no significant interference from other species, while ratios of ϕ greater than 1.0 imply the role of other peroxy radical species (e.g., RO_2, HO_2) in the conversion of NO to NO_2 (Pitts and Finlayson-Pitts, 2000). The NO_2/NO ratios were obtained from the NO_x analyzer measurements, O_3 mixing ratios were obtained from local monitoring stations during the same daytime periods as the transects. Values of j_{NO2} were estimated using SLEA Moore Line station solar irradiance data (Fig. 1; Table S1) and solar zenith angle following the method in Wiegand and Bofinger (2000).

Table 2 shows Leighton ratios calculated at the locations of maximum NO_2 VCD enhancements. Calculated Leighton ratios were significantly greater than 1 (ϕ = 1.7-2.3) at peak NO_x locations on Day 1 (Table 2). Even if we consider a potential bias of + 20% in the NO_2 measurements by the NO_x analyzer for reasons outlined in Section 3.2 (highly unlikely in a fresh NO_x plume), a +20% bias in the Leighton ratio would still give (ϕ = 1.4-1.9). We interpret this as an indication that significant levels of peroxy radicals were present in the plume, presumably from VOC oxidation by the OH radical. This is consistent with high VOC emissions from the petrochemical facilities in Sarnia, with emission rates >300 tonnes yr^{-1} each for four of the top six industrial NO_x emitters in Sarnia (Environment and Climate Change Canada, 2018d). The Day 2 Leighton ratio of less than 1.0 in Table 2 suggests a relatively fresh plume (only 4 km downwind of a facility) that had not come to photo-stationary state.

Thus we have indications that OH production may be lower than summer time leading to longer NOx lifetimes and we have indications that VOC oxidation in the plume may be significant leading to shorter NOx lifetimes than air masses where the photo-stationary state in NO_x is valid. Without further information, we have opted to assume a central NO_x lifetime assume of ~ 6 hr. Sensitivity calculations were conducted for NO_x emission estimates using a

range of lifetimes of 4-8 hours (Supplement S7). Varying the lifetime from ± 2 hours changed the emission estimates by <15% for all routes except for Day 1 route 1 due to low wind-speeds during that route (30% change).

For the calculation of SO_2 emissions, SO_2 was assumed to have a sufficiently long lifetime in the boundary layer so as to be conserved between the emission and measurement location. Note that cloud processing of SO_2 was assumed to be negligible since SO_2 measurements were completed on a mostly cloud-free day.

3.4 Emission Estimates

3.4.1 Emission Estimates of Sarnia

The VCDs measured are shown in Fig. 3-6 while the NO_x emissions calculated using Eqs. (3) and (4) are shown in Table 4. The values of VCD_{influx} required for the calculations were typically determined from measurements of VCD in low pollution transect areas. However, the VCD_{influx} on Day 2 was not determined in this way since these DSCDs were close to zero within error (Figs. 2 & 4). The VCD_{influx} is expected to be low on Day 2 because the north wind-direction indicates that the air-masses originated from over Lake Huron. These low values were probably due to low light levels during measurement, insufficiently long integration times (low signal to noise ratio) and NO_2 background VCD values below the instrument's limit of detection. A low value of $VCD_{influx} = 0.5(\pm 0.5)\times 10^{15}$ molec cm^{-2} was therefore assumed.

The emissions were calculated in two ways i) using a route-average NO_x/NO_2 ratio value for each route estimate and ii) using individual NO_x/NO_2 ratios co-located with each VCD measurement. For Day 1 route, the route average NO_x/NO_2 ratio was 1.53 ± 0.12 ppb ppb^{-1} with the difference between the calculated emission rates using the two methods being only 3%. Day 1 transects 2-4 exhibited small variability in NO_x/NO_2 (Table 4) and the variation in the NO_x/NO_2 ratio impacted emission estimates by less than 5%.

However, the difference between emission estimates calculated using individual NO_x/NO_2 ratios versus a route-averaged value can be non-trivial, as observed with the Day 2 route 1. Day 2 had consistent northerly wind conditions, and east-west transects were driven south of Sarnia to capture the urban plume and background regions to the east (Fig. 4). The resultant Sarnia NO_x emission using the first method is consistent with the first three Day 1 emission estimates but the application of the second method (individual NO_x/NO_2 ratios collocated with each VCD)

increased the emission estimate by ~50% (Table 4 and Fig. 8). The NO_x/NO_2 ratio was generally consistent with the averaged value of 1.3 (maximum NO_x/NO_2 removed) but increased to 3 in the region of maximum NO_2 VCD enhancements 7 km south of the NOVA Chemicals facility (Table 3). The calculated Leighton ratio for this peak NO_x/NO_2 ratio location is less than 1 (see 3.4.2 and Table 3). The Leighton ratio suggests the plume from the NOVA Chemical facility had significant NO that had not had sufficient time to come to a photostationary state. The emission estimate using individual NO_x/NO_2 ratios is considered the more accurate value for this route compared to the emission value calculated using the route-averaged ratio.

The importance of measuring the local NO_x/NO_2 ratio is also illustrated by observing variation of the ratio due to the impact of the Michigan power-plants' plume, apparent in the Day 1 route 1 East-West transect (Fig. 3a). The NO_x/NO_2 ratio along this transect increased to ~1.7 (Fig. 7), higher than the maximum NO_x/NO_2 ratio observed in the North-South transect downwind of Sarnia. A higher ratio is somewhat unexpected because the distance between the source and receptor measurement for the power plant source was greater than the source-receptor distance for the Sarnia sources. Thus, the power-plant plume would have been expected to be more aged, but the results suggest that the power-plants' plumes had a slower conversion of NO to NO_2 perhaps due to higher initial mixing ratios of NO_x (Nunnermacker et al., 2000). Very high NO mixing ratios in a power plant plume (i.e., > 40ppb) could completely titrate the ambient O_3 in the air entrained into the plume, an observation previously seen in power plant plumes (Brown et al., 2012).

The East-West transect appears to have captured approximately half of the power-plants' plume since the NO_2 VCDs and the NO_2 mixing ratios increase from background to a plateau at a maximum (Fig. 2a). A preliminary estimation of the NO_x and SO_2 emissions from the power-plants can be determined by scaling up the flux integral from the appropriate section of the East-West transect by a factor of two . While this is highly uncertain, we do this to make a first order estimate of the power plant plumes on the US side of the border. In this case, we have used VCD_{influx} = 2-3×10^{15} molec cm^{-2} for NO_x and zero for SO_2 since the background region SO_2 DSCDs were at or below detection limits. The NO_x estimate used individual NO_x/NO_2 ratios because the NO_x/NO_2 ratio was significantly higher in the plume than outside the plume. This illustrates the importance of in-situ instruments of NO_x/NO_2, especially when close to the source where plume NO_x/NO_2 ratios can be variable (Valin et al., 2013). Given the above assumptions, a tentative first order estimate of the total emissions from the power plants are 0.31-

0.46 tonnes NO_x hr^{-1} and 0.77 tonnes SO_2 hr^{-1}, respectively. The hourly emissions of the power-plants from reported 2015 annual values are 0.74 tonnes NO_x hr^{-1} and 2.56 tonnes SO_2 hr^{-1} (United States EPA, 2018). Our hourly estimates are only preliminary since only half of the plume (approximately) was captured by the measurement transect.

The NO_x emission estimates from Sarnia from Day 1 are consistent within 25% and are consistent with the Day 2 estimates within the calculated error of approximately ±45% (Fig. 8, Table 4). Some variability between the emission estimates is expected due to wind-data uncertainties, NO_x/NO_2 vertical profile variability, errors introduced by using a constant VCD_{influx} and NO_x lifetime, and temporal variations in emissions from the source.

Conversion of the hourly measured emissions to annual emissions would require knowledge and application of daily, weekly and seasonal emission profiles, which is beyond the scope of this work. The Mobile-MAX-DOAS emission estimates are reported in units of tonnes per hour since routes were completed within <40 minutes. Events such as flaring can significantly increase the instantaneous emission rate but are excluded from the annual emission inventory data. However, there was no reported flaring during the measurement period (MOECC 2017; personal communication). NO_x emissions from petrochemical facilities, excluding flaring, typically have low variability during periods of continuous operation. According to Ryerson et al. (2003), variation in average hourly NO_x emissions from a petrochemical facility reported by industry (CEMS data) was <10% from an average of the hourly average emissions over 11 days in Houston, Texas. However, this trend may be different for the chemical industry. A first-order comparison to the 2017 National Pollution Release Inventory (NPRI) values (downscaled by assuming constant emissions) was made to determine whether our measured Sarnia emissions are reasonable. The NPRI value is the sum of the NO_x emissions from the top 9 industrial emitters of NO_x in Sarnia whose emissions would have been captured along the driving routes. The NPRI requires significant point source industry facilities to report their pollutant emissions, but the method of estimating emissions can vary by facility (ECCC, 2015). The NPRI emission value does not include mobile and area sources from the Sarnia region. Thus, the NPRI emission inventory values for Sarnia would be expected to be smaller than our measured emissions because of this exclusion. The measured NO_x emissions are larger than the 2017 NPRI value but not statistically so (Fig. 8; Table 4). The exception is the Day 1 route 1* value, which is statistically higher. The average of the four NO_x emission estimates from Sarnia is greater than the 2017 NPRI value. These results demonstrate that our measured emission rates are reasonable. Future

Mobile-MAX-DOAS studies could focus on determining diurnal trends in emissions by driving multiple routes at as many times of the day as possible on multiple days, seasons and weekdays/weekends. Measurements of vertical wind profiles could reduce emission uncertainty to allow identification of temporal trends by comparing same-day measurements.

Apart from NO_x, we were also able to estimate SO_2 emissions from the Sarnia urban/industrial region during one route when the SO_2 DSCDs were detectable, Day 1 route 3 (Table 5). Our SO_2 emission estimate using the 10 m wind-speed is consistent within error with the 2017 NPRI value (Table 5). We expect our SO_2 emission estimate to be closer to the NPRI values compared to the NO_x estimates because SO_2 emissions from area and mobile sources in Sarnia are expected to be small relative to industrial sources (Ministry of the Environment and Climate Change, 2016). Since ships were not operating in the St. Clair River at this time of year, shipping emissions of SO_2 were absent. Thus SO_2 plumes in this region are localized to the major industrial emissions sources. Therefore, the VCDs from the areas unaffected by the Sarnia plumes are representative of background values, VCD_{influx}. While the Mobile-MAX-DOAS was able to capture these plumes (Fig. 9), only 1 of 7 local monitoring stations (LaSalle Road, Fig. S1) observed elevated levels of SO_2 during this period. The under-sampling by stations is due to the highly localized nature of the SO_2 plumes that are from stacks where the plume is frequently elevated above the surface. These results illustrate the complementary nature of Mobile-MAX-DOAS and in-situ measurements and the importance of monitoring techniques that can capture localized plumes independent of the wind direction.

3.4.2 Emission Estimates of NOVA Chemicals Industrial Facility

NO_x emissions were opportunistically measured from a single facility on Day 3 because the southerly wind-directions isolated this plume (Environment and Climate Change Canada, 2018b) from other industrial sources in Sarnia. The plume originated from Nova Chemicals, the 2nd highest emitter of NO_x in the region in 2017. These conditions allowed us to test the mobile-MAX-DOAS method in isolating a single plume. The wind-direction on Day 3 indicated that the air-masses originated from rural areas south of Sarnia and the VCD_{influx} was expected to be low, ~ 1×10^{15} molec cm^{-2}.

The emission estimates of NO_x from the two routes on Day 3 from the NOVA Chemicals industrial site (Tables 4 & 5) are consistent with each other within 10%. The consistency increases confidence in fitting the spectra in each

transect against a local FRS and removing influx using the average "background" VCDs rather than using the "$DSCD_{Offset}$" method in this case. The use of "background" VCDs is appropriate because vehicular traffic upwind of the measurement transect is minimal in the local area. Upwind emissions were unlikely to have contributed significantly to the total measured emissions. The emission estimates from NOVA Chemicals are larger than the 2017 NPRI value (Tables 4 & 5). This comparison merely indicates that the Mobile-MAX-DOAS values are reasonable given that there was likely diurnal variability and the measurements were taken only during a single hour on a single day.

3.5 Comparison of OMI Satellite and MAX-DOAS VCDs

The satellite and MAX-DOAS NO_2 VCDs on Day 1 exhibit similar spatial trends in the simple sense that NO_2 VCDs increase towards the south from the background regions north of Sarnia (Fig. 10). This trend is probably due to a combination of emissions from U.S.A. power-plants, the Detroit area as well as Sarnia. The NO_2 VCD of the pixel containing the majority of the Sarnia industrial facilities is comparable to rural area VCDs to the north-west of Sarnia. Only $1/8^{th}$ of the "Sarnia" pixel's footprint region is likely to be impacted by Sarnia emissions, and the remainder observes mostly rural to semi-rural regions. The OMI Pixel from Day 3 (Fig. 11) containing Sarnia exhibits a minimal increase in NO_2 VCD ($1\text{-}2\times10^{15}$ molec cm^{-2}) compared to the surrounding background regions (Fig. 11). In contrast, the Mobile-MAX-DOAS measurements observed VCD enhancements of up to 1×10^{16} molec cm^{-2} within this pixel. The averaging due by the large pixel size (24 km×84 km) causes underestimation of the maximum VCDs. Identification of Sarnia-only emissions without error due to horizontal averaging or inclusion of other sources may require satellite measurements with nadir-viewing pixels centred on Sarnia and/or extremely large averaging times.

3.6 Uncertainties in this Study and Recommended Improvements for Mobile-MAX-DOAS Measurements

Many of the factors that increased the uncertainty in the emission values in this study can be significantly reduced in future through relatively small changes in the method. The many factors have been addressed in Supplemental Information (section S7) and summarized in Table S9. Ideally accurate horizontal flux measurements would require knowledge of the vertical and horizontal profile of pollutant concentrations as well as the vertical and horizontal profile of wind vectors. Lack of knowledge of the vertical profile of wind-speed increases uncertainty in Mobile-

MAX-DOAS emission estimates since elevated plumes and well-mixed plumes are transported by winds with typically higher speeds than those near the surface. Future studies could focus on reducing uncertainty by using measurements from sodar, lidar, tall towers, balloon soundings, or a radio acoustic meteorological profiler. In this study, uncertainty was increased (18-30% based on sensitivity analysis; see supplementary S5 & S7) because driving routes could not always include measurements along influx regions (Day 1) due to road proximity to sources or obstructions to the viewing field. Future experiments could measure influx values while stationary at multiple locations along the upwind region chosen for an unobstructed viewing field. Very low background trace-gas levels also resulted in SO_2 DSCDs that were below detection limit most of the time, while being occasionally below detection limit for NO_2 (Fig. 2e). A spectrometer with higher sensitivity giving lower detection limits could solve this issue. Increased averaging of spectra would also improve detectability but at the expense of worse spatial resolution, unless measurements can be made at a slower driving speed. Uncertainty in the NO_x lifetime was a small contribution to uncertainty in this study (up to ±12%) because the distances and transport times between source and measurement locations were relatively small (<25 km). The exception was Day 1 route 1 where uncertainty was up to 30% due to low wind-speeds. The error contribution of NO_x lifetime could be non-trivial if driving routes are far from the sources (e.g., large cities). This error could also be non-trivial if the lifetime that one assumes does not account for the multiple factors discussed in Section 3.3. Bias in the emission estimates from an incorrect lifetime could be avoided by determining NO_x lifetimes from photochemical modelling or, for large cities, satellite observations (Beirle et al., 2011) but taking into account wind speeds (Valin et al., 2013).

4 Conclusions

In this study, we combined Mobile-MAX-DOAS techniques with mobile NO_x measurements and a modular meteorological station to measure emissions of NO_x and SO_2 from the Sarnia region, a relatively small urban/industrial city. Trace-gas VCDs were determined using the $DSCD_{offset}$ method (Wagner et al., 2010) or by fitting measured spectra against a route-local low pollution spectrum. Both methods provided good results, which suggest that the first method is ideal if there are many hours of measurements while the second method is ideal when short routes contain low-pollution regions. Average lower limit Mobile-MAX-DOAS emissions of NO_x from Sarnia were measured to be 1.60 ± 0.34 tonnes hr^{-1} using 10 m elevation measured wind-speeds. The estimates were larger than the downscaled 2017 NPRI reported industrial emissions of 0.9 tonnes hr^{-1} (Environment and Climate Change Canada, 2018b) but the NPRI estimate excludes area and mobile emissions. Our lower limit SO_2 emission

measurement for Sarnia was 1.81 ± 0.83 tonnes hr^{-1} using 10 m wind-speeds, which is equal within uncertainty to the 2017 NPRI value of 1.85 tonnes hr^{-1} (Environment and Climate Change Canada, 2018c). Our average lower limit NO_x emission measurement from the NOVA Chemicals Facility was 0.28 ± 0.06 tonnes hr^{-1}, the same order of magnitude as the 2016 NPRI value of 0.14 tonnes hr^{-1} (Environment and Climate Change Canada, 2018a).

Simultaneous measurements of NO-NO_2-NO_x improved the accuracy of NO_x emission estimates when plumes of varying ages were observed. The NO_x results from Days 1 and 2 suggest that accurate Mobile-MAX-DOAS NO_x emission measurements from routes that observe plumes with differing ages require accurate knowledge of the localized NO_x/NO_2 ratio.

The variability in the ratio of the NO_2 VCDs and mixing ratios indicates that surface NO_2 mixing ratios cannot be reliably estimated from NO_2 VCDs and boundary layer height alone when pollution is emitted from sources of varying heights and chemical composition. A NO_x-analyzer can be an essential component of Mobile-MAX-DOAS NO_2 measurements. The addition of this instrument allows the method to characterize the boundary layer fully and accurately estimate NO_x emissions from NO_2 measurements when multiple NO_x sources are present and when transects are sufficiently distant from the sources.

The modular meteorological station improved knowledge of local wind essential to identify time periods of low temporal variability, ensuring low error due to wind estimation. These time periods would have been difficult to identify with only hourly average or modelled wind data. Accurate knowledge of the vertical wind profile would significantly enhance the accuracy of the Mobile-MAX-DOAS emission estimates. Future studies could obtain vertical wind profiles using sodar, lidar, wind-rass, and radiosonde on a weather balloon or local aircraft soundings.

Mobile-MAX-DOAS measurements identified significant OMI intrapixel inhomogeneity and observed industrial pollution enhancements that were poorly captured by the in-situ ground stations. These results suggest that Mobile-MAX-DOAS has clear advantages in similar industrial regions over other remote sensing techniques used for estimating emissions (e.g., using aircraft or satellite): higher spatial resolution, the potential for multiple emission estimates per day (i.e., observations of diurnal trends), and much lower operational costs. Mobile-MAX-DOAS is a "top-down" low-cost solution for validating bottom-up inventories that compliments in-situ monitoring and has

significant utility in smaller regions with significant emissions where satellite applications are limited. Future Mobile-MAX-DOAS studies in such regions can focus on measuring temporal trends in emissions.

Author Contributions

ZD conceived of and organized the field campaign with aid from RM. ZD, SB, AK, WF, CC and RM carried out the experiments in Sarnia. CM modelled conditions for the satellite retrievals of NO_2 in the region of Sarnia, and provided useful advice. ZD and RM prepared the manuscript, with contributions from all co-authors.

Acknowledgements

This study was completed with collaborative support by the Ontario Ministry of the Environment and Climate Change. Funding for the study was provided by NSERC, CREATE IACPES and the York University Faculty of Graduate Studies. The corresponding author would like to thank Mr. Barry Duffey at the Ontario Ministry of Environment and Climate Change for his support at the project start. We also thank Tony Munoz of OME for his continued support of our research.

References

Alicke, B., Platt, U., and Stutz, J.: Impact of nitrous acid photolysis on the total hydroxyl radical budget during the limitation of oxidant production/Pianura Padana Produzione di Ozono study in Milan, J. Geophys. Res., 107(D22), 8196,doi:10.1029/2000JD000075, 2002.

Baray, S., Darlington, A., Gordon, M., Hayden, K. L., Leithead, A., Li, S.-M., Liu, P. S. K., Mittermeier, R. L., Moussa, S. G., O'Brien, J., Staebler, R., Wolde, M., Worthy, D. and McLaren, R.: Quantification of methane sources in the Athabasca Oil Sands Region of Alberta by aircraft mass balance, Atmospheric Chem. Phys., 18(10), 7361–7378, doi:10.5194/acp-18-7361-2018, 2018.

Beirle, S., Boersma, K. F., Platt, U., Lawrence, M. G. and Wagner, T.: Megacity Emissions and Lifetimes of Nitrogen Oxides Probed from Space, Science, 333(6050), 1737–1739, doi:10.1126/science.1207824, 2011.

Boersma, K. F., Eskes, H. J., Veefkind, J. P., Brinksma, E. J., Van der A, R. J., Sneep, M., van den Oord, G. H. J., Levelt, P. F., Stammes, P., Gleason, J. F. and Bucsela, E. J.: Near-real time retrieval of tropospheric NO2 from OMI, Atmospheric Chem. Phys., 7(8), 2103–2118, 2007.

Bogumil, K., Orphal, J., Homann, T., Voigt, S., Spietz, P., Fleischmann, O. C., Vogel, A., Hartmann, M., Kromminga, H., Bovensmann, H., Frerick, J. and Burrows, J. P.: Measurements of molecular absorption spectra with the SCIAMACHY pre-flight model: instrument characterization and reference data for atmospheric remote-sensing in the 230-2380 nm region, J. Photochem. Photobiol. Chem., 157(2–3), 167–184, doi:10.1016/S1010-6030(03)00062-5, 2003.

Brinksma, E. J., Pinardi, G., Volten, H., Braak, R., Richter, A., Schoenhardt, A., van Roozendael, M., Fayt, C., Hermans, C., Dirksen, R. J., Vlemmix, T., Berkhout, A. J. C., Swart, D. P. J., Oetjen, H., Wittrock, F., Wagner, T., Ibrahim, O. W., de Leeuw, G., Moerman, M., Curier, R. L., Celarier, E. A., Cede, A., Knap, W. H., Veefkind, J. P., Eskes, H. J., Allaart, M., Rothe, R., Piters, A. J. M. and Levelt, P. F.: The 2005 and 2006 DANDELIONS NO_2 and

aerosol intercomparison campaigns, J. Geophys. Res.-Atmospheres, 113(D16), D16S46, doi:10.1029/2007JD008808, 2008.

Brown, S. S., Dube, W. P., Karamchandani, P., Yarwood, G., Peischl, J., Ryerson, T. B., Neuman, J. A., Nowak, J. B., Holloway, J. S., Washenfelder, R. A., Brock, C. A., Frost, G. J., Trainer, M., Parrish, D. D., Fehsenfeld, F. C. and Ravishankara, A. R.: Effects of NO_x control and plume mixing on nighttime chemical processing of plumes from coal-fired power plants, J. Geophys. Res.-Atmospheres, 117, D07304, doi:10.1029/2011JD016954, 2012.

ECCC, Environment and Climate Change Canada.: Using and interpreting data from the National Pollutant Release Inventory, aem [online] Available from: https://www.canada.ca/en/environment-climate-change/services/national-pollutant-release-inventory/using-interpreting-data.html (Accessed 1 August 2018), 2015.

Davis, Z. Y. W., Frieβ, U., Strawbridge, K. B., Aggarwaal, M., Baray, S., Schnitzler, E. G., Lobo, A., Fioletov, V. E., Abboud, I., McLinden, C. A., Whiteway, J., Willis, M. D., Lee, A. K. Y., Brook, J., Olfert, J., O'Brien, J., Staebler, R., Osthoff, H. D., Mihele, C., and McLaren, R.: Validation of MAX-DOAS retrievals of aerosol extinction, SO_2 and NO_2 through comparison with lidar, sun photometer, Active-DOAS and aircraft measurements in the Athabasca Oil Sands Region, Atmos. Meas. Tech. Discuss., https://doi.org/10.5194/amt-2019-296, in review, 2019.

Dragomir, C. M., Constantin, D.-E., Voiculescu, M., Georgescu, L. P., Merlaud, A. and Van Roozendael, M.: Modeling results of atmospheric dispersion of NO_2 in an urban area using METI-LIS and comparison with coincident mobile DOAS measurements, Atmos. Pollut. Res., 6(3), 503–510, doi:10.5094/APR.2015.056, 2015.

Dunlea, E. J., Herndon, S. C., Nelson, D. D., Volkamer, R. M., San Martini, F., Sheehy, P. M., Zahniser, M. S., Shorter, J. H., Wormhoudt, J. C., Lamb, B. K., Allwine, E. J., Gaffney, J. S., Marley, N. A., Grutter, M., Marquez, C., Blanco, S., Cardenas, B., Retama, A., Ramos Villegas, C. R., Kolb, C. E., Molina, L. T., and Molina, M. J.: Evaluation of nitrogen dioxide chemiluminescence monitors in a polluted urban environment, Atmos. Chem. Phys., 7, 2691-2704, 10.5194/acp-7-2691-2007, 2007.

Environment and Climate Change Canada: NPRI Data Search - Facility and Substance Information - NOVA Chemicals (Canada) Ltd. - Corunna Site 2017, [online] Available from: https://pollution-waste.canada.ca/national-release-inventory/archives/index.cfm (Accessed 17 September 2018a), 2018.

Environment and Climate Change Canada: NPRI Data Search - Facility Search Results Nitrogen oxides (expressed as NO2) (11104-93-1), [online] Available from: https://pollution-waste.canada.ca/national-release-inventory/archives/index.cfm (Accessed 17 September 2018b), 2018.

Environment and Climate Change Canada: NPRI Data Search - Facility Search Results Sulphur Dioxide (7446-09-5), [online] Available from: https://pollution-waste.canada.ca/national-release-inventory/archives/index.cfm (Accessed 17 September 2018c), 2018.

Environment and Climate Change Canada: NPRI Facility Search Results - Volatile Organic Compounds (VOCs) (NA-M16), [online] Available from: https://pollution-waste.canada.ca/national-release-inventory/archives/index.cfm (Accessed 17 September 2018d), 2018.

Finlayson-Pitts, B. J. and Pitts, J.N.: Chemistry of the Upper and Lower Atmosphere, Academic Press, San Diego CA, 969 pp., 2000.

Friess, U., Monks, P. S., Remedios, J. J., Rozanov, A., Sinreich, R., Wagner, T. and Platt, U.: MAX-DOAS O4 measurements: A new technique to derive information on atmospheric aerosols: 2. Modeling studies, J. Geophys. Res.-Atmospheres, 111(D14), D14203, doi:10.1029/2005JD006618, 2006.

Gordon, M., Li, S.-M., Staebler, R., Darlington, A., Hayden, K., O'Brien, J. and Wolde, M.: Determining air pollutant emission rates based on mass balance using airborne measurement data over the Alberta oil sands operations, Atmos. Meas. Tech., 8(9), 3745–3765, doi:10.5194/amt-8-3745-2015, 2015.

627 Halla, J. D., Wagner, T., Beirle, S., Brook, J. R., Hayden, K. L., O'Brien, J. M., Ng, A., Majonis, D., Wenig, M. O.
628 and McLaren, R.: Determination of tropospheric vertical columns of NO2 and aerosol optical properties in a rural
629 setting using MAX-DOAS, Atmos. Chem. Phys., 11(23), 12475–12498, doi:10.5194/acp-11-12475-2011, 2011.

630 Heckel, A., Richter, A., Tarsu, T., Wittrock, F., Hak, C., Pundt, I., Junkermann, W. and Burrows, J. P.: MAX-DOAS
631 measurements of formaldehyde in the Po-Valley, Atmos. Chem. Phys., 5, 909–918, doi:10.5194/acp-5-909-2005,
632 2005.

633 Heckel, A., Kim, S.-W., Frost, G. J., Richter, A., Trainer, M. and Burrows, J. P.: Influence of low spatial resolution
634 a priori data on tropospheric NO_2 satellite retrievals, Atmos. Meas. Tech., 4(9), 1805–1820, doi:10.5194/amt-4-
635 1805-2011, 2011.

636 Honninger, G. and Platt, U.: Observations of BrO and its vertical distribution during surface ozone depletion at
637 Alert, Atmos. Environ., 36(15–16), 2481–2489, doi:10.1016/S1352-2310(02)00104-8, 2002.

638 Honninger, G., von Friedeburg, C. and Platt, U.: Multi axis differential optical absorption spectroscopy (MAX-
639 DOAS), Atmos. Chem. Phys., 4, 231–254, 2004.

640 Huang, M., Bowman, K. W., Carmichael, G. R., Chai, T., Pierce, R. B., Worden, J. R., Luo, M., Pollack, I. B.,
641 Ryerson, T. B., Nowak, J. B., Neuman, J. A., Roberts, J. M., Atlas, E. L. and Blake, D. R.: Changes in nitrogen
642 oxides emissions in California during 2005-2010 indicated from top-down and bottom-up emission estimates, J.
643 Geophys. Res.-Atmospheres, 119(22), 12928–12952, doi:10.1002/2014JD022268, 2014.

644 Ialongo, I., Hakkarainen, J., Hyttinen, N., Jalkanen, J.-P., Johansson, L., Boersma, K. F., Krotkov, N. and
645 Tamminen, J.: Characterization of OMI tropospheric NO2 over the Baltic Sea region, Atmos. Chem. Phys., 14(15),
646 7795–7805, doi:10.5194/acp-14-7795-2014, 2014.

647 Ialongo, I., Herman, J., Krotkov, N., Lamsal, L., Boersma, K. F., Hovila, J. and Tamminen, J.: Comparison of OMI
648 NO2 observations and their seasonal and weekly cycles with ground-based measurements in Helsinki, Atmos. Meas.
649 Tech., 9(10), 5203–5212, doi:10.5194/amt-9-5203-2016, 2016.

650 Ibrahim, O., Shaiganfar, R., Sinreich, R., Stein, T., Platt, U. and Wagner, T.: Car MAX-DOAS measurements
651 around entire cities: quantification of NOx emissions from the cities of Mannheim and Ludwigshafen (Germany),
652 Atmos. Meas. Tech., 3(3), 709–721, doi:10.5194/amt-3-709-2010, 2010.

653 Irie, H., Kanaya, Y., Akimoto, H., Iwabuchi, H., Shimizu, A. and Aoki, K.: First retrieval of tropospheric aerosol
654 profiles using MAX-DOAS and comparison with lidar and sky radiometer measurements, Atmos. Chem. Phys.,
655 8(2), 341–350, doi:10.5194/acp-8-341-2008, 2008.

656 Kim, N. K., Kim, Y. P., Morino, Y., Kurokawa, J. and Ohara, T.: Verification of NOx emission inventories over
657 North Korea, Environ. Pollut., 195, 236–244, doi:10.1016/j.envpol.2014.06.034, 2014.

658 Leighton, P. A.: Photochemistry of air pollution. --, Academic Press, New York., 1961.

659 Liu, F., Beirle, S., Zhang, Q., Doerner, S., He, K. and Wagner, T.: NOx lifetimes and emissions of cities and power
660 plants in polluted background estimated by satellite observations, Atmos. Chem. Phys., 16(8), 5283–5298,
661 doi:10.5194/acp-16-5283-2016, 2016.

662 McLinden, C. A., Fioletov, V., Boersma, K. F., Krotkov, N., Sioris, C. E., Veefkind, J. P. and Yang, K.: Air quality
663 over the Canadian oil sands: A first assessment using satellite observations, Geophys. Res. Lett., 39, L04804,
664 doi:10.1029/2011GL050273, 2012.

665 Ministry of the Environment and Climate Change: Air Quality in Ontario 2014 Report, 2015. [online] Available
666 from: https://www.ontario.ca/page/air-quality-ontario-2014-report (Accessed 17 Sept. 2019).

Ministry of the Environment and Climate Change: Air Quality in Ontario 2016 Report., 2017. [online] Available from: https://www.ontario.ca/document/air-quality-ontario-2016-report (Accessed 17 Sept. 2019).

Nunnermacker, L. J., Kleinman, L. I., Imre, D., Daum, P. H., Lee, Y.-N., Lee, J. H., Springston, S. R., Newman, L. and Gillani, N.: NO y lifetimes and O3 production efficiencies in urban and power plant plumes: Analysis of field data, J. Geophys. Res. Atmospheres, 105(D7), 9165–9176, doi:10.1029/1999JD900753, 2000.

Oiamo, T. H., Luginaah, I. N., Atari, D. O. and Gorey, K. M.: Air pollution and general practitioner access and utilization: a population based study in Sarnia, `Chemical Valley,' Ontario, Environ. Health, 10, doi:10.1186/1476-069X-10-71, 2011.

Platt, U., Perner, D. and Patz, H.: Simultaneous Measurement of Atmospheric CH_2O, O_3, and NO_2 by Differential Optical-Absorption, J. Geophys. Res.-Oceans Atmospheres, 84(NC10), 6329–6335, doi:10.1029/JC084iC10p06329, 1979.

Platt, U., Perner, D., Harris, G.W.,Winer, A. M., and Pitts Jr., J. N.: Observations of nitrous acid in an urban atmosphere by differential optical absorption, Nature, 285, 312–314, 1980.

Platt, U., Stutz, J., Springer E-books - York University and SpringerLink (Online service): Differential optical absorption spectroscopy: principles and applications, Springer Verlag, Berlin. [online] Available from: http://www.library.yorku.ca/eresolver/?id=1261530, 2008.

Rivera, C., Mellqvist, J., Samuelsson, J., Lefer, B., Alvarez, S., and Patel, M. R.: Quantification of NO_2 and SO_2 emissions from the Houston Ship Channel and Texas City industrial areas during the 2006 Texas Air Quality Study, Journal of Geophysical Research: Atmospheres, 115, 10.1029/2009jd012675, 2010.

Ryerson, T. B., Trainer, M., Angevine, W. M., Brock, C. A., Dissly, R. W., Fehsenfeld, F. C., Frost, G. J., Goldan, P. D., Holloway, J. S., Hubler, G., Jakoubek, R. O., Kuster, W. C., Neuman, J. A., Nicks, D. K., Parrish, D. D., Roberts, J. M., Sueper, D. T., Atlas, E. L., Donnelly, S. G., Flocke, F., Fried, A., Potter, W. T., Schauffler, S., Stroud, V., Weinheimer, A. J., Wert, B. P., Wiedinmyer, C., Alvarez, R. J., Banta, R. M., Darby, L. S. and Senff, C. J.: Effect of petrochemical industrial emissions of reactive alkenes and NOx on tropospheric ozone formation in Houston, Texas, J. Geophys. Res.-Atmospheres, 108(D8), 4249, doi:10.1029/2002JD003070, 2003.

Seinfeld, J. H. and Pandis, S. N.: Atmospheric Chemistry and Physics: From Air Pollution to Climate Change, John Wiley & Sons., 2006.

Shabbir, Y., Khokhar, M. F., Shaiganfar, R. and Wagner, T.: Spatial variance and assessment of nitrogen dioxide pollution in major cities of Pakistan along N5-Highway, J. Environ. Sci., 43(Supplement C), 4–14, doi:10.1016/j.jes.2015.04.038, 2016.

Shaiganfar, R., Beirle, S., Sharma, M., Chauhan, A., Singh, R. P. and Wagner, T.: Estimation of NOx emissions from Delhi using Car MAX-DOAS observations and comparison with OMI satellite data, Atmos. Chem. Phys., 11(21), 10871–10887, doi:10.5194/acp-11-10871-2011, 2011.

Shaiganfar, R., Beirle, S., Petetin, H., Zhang, Q., Beekmann, M. and Wagner, T.: New concepts for the comparison of tropospheric NO2 column densities derived from car-MAX-DOAS observations, OMI satellite observations and the regional model CHIMERE during two MEGAPOLI campaigns in Paris 2009/10, Atmos. Meas. Tech., 8(7), 2827–2852, doi:10.5194/amt-8-2827-2015, 2015.

Shaiganfar, R., Beirle, S., van der Gon, H. D., Jonkers, S., Kuenen, J., Petetin, H., Zhang, Q., Beekmann, M. and Wagner, T.: Estimation of the Paris NOx emissions from mobile MAX-DOAS observations and CHIMERE model simulations during the MEGAPOLI campaign using the closed integral method, Atmos. Chem. Phys., 17(12), 7853–7890, doi:10.5194/acp-17-7853-2017, 2017.

Tokarek, T. W., Odame-Ankrah, C. A., Huo, J. A., McLaren, R., Lee, A. K. Y., Adam, M. G., Willis, M. D., Abbatt, J. P. D., Mihele, C., Darlington, A., Mittermeier, R. L., Strawbridge, K., Hayden, K. L., Olfert, J. S., Schnitzler, E. G., Brownsey, D. K., Assad, F. V., Wentworth, G. R., Tevlin, A. G., Worthy, D. E. J., Li, S.-M., Liggio, J., Brook, J. R. and Osthoff, H. D.: Principal component analysis of summertime ground site measurements in the Athabasca oil sands with a focus on analytically unresolved intermediate volatility organic compounds, Atmos. Chem. Phys., 2018, 17819-17841, doi:10.5194/acp-18-17819-2018, 2018.

United States EPA: Air Pollutant Report | ECHO | US EPA, Air Pollut. Rep. [online] Available from: https://echo.epa.gov/air-pollutant-report?fid=110000404740 (Accessed 2 August 2018), 2018.

Valin, L. C., Russell, A. R. and Cohen, R. C.: Variations of OH radical in an urban plume inferred from NO_2 column measurements, Geophys. Res. Lett., 40(9), 1856–1860, doi:10.1002/grl.50267, 2013.

Wagner, T., Dix, B., von Friedeburg, C., Friess, U., Sanghavi, S., Sinreich, R. and Platt, U.: MAX-DOAS O-4 measurements: A new technique to derive information on atmospheric aerosols - Principles and information content, J. Geophys. Res.-Atmospheres, 109(D22), D22205, doi:10.1029/2004JD004904, 2004.

Wagner, T., Ibrahim, O., Shaiganfar, R. and Platt, U.: Mobile MAX-DOAS observations of tropospheric trace gases, Atmos. Meas. Tech., 3(1), 129–140, 2010.

Wagner, T., Beirle, S., Brauers, T., Deutschmann, T., Friess, U., Hak, C., Halla, J. D., Heue, K. P., Junkermann, W., Li, X., Platt, U. and Pundt-Gruber, I.: Inversion of tropospheric profiles of aerosol extinction and HCHO and NO2 mixing ratios from MAX-DOAS observations in Milano during the summer of 2003 and comparison with independent data sets, Atmos. Meas. Tech., 4(12), 2685–2715, doi:10.5194/amt-4-2685-2011, 2011.

Wiegand, A. N. and Bofinger, N. D.: Review of empirical methods for the calculation of the diurnal NO2 photolysis rate coefficient, Atmos. Environ., 34(1), 99–108, doi:10.1016/S1352-2310(99)00294-0, 2000.

Wu, F., Li, A., Xie, P., Chen, H., Hu, Z., Zhang, Q., Liu, J. and Liu, W.: Emission Flux Measurement Error with a Mobile DOAS System and Application to NOx Flux Observations, Sensors, 17(2), doi:10.3390/s17020231, 2017.

Table 1 Daily meteorological conditions, number of routes and time period of routes driven. Wind-speed from SLEA LaSalle Road; Temperature and Relative Humidity from portable meteorological station Day 1 and Day 2 and from Moore Line station Day 2.

Date	Number of Routes Driven	Measurement Local Time Period	Average Wind-speed ($km\,hr^{-1}$)	Prevailing Wind-Direction	Average Temperature (^oC)	Average Relative Humidity (%)	Emission Area Measured
3/21/2017	4	10:26-13:16	15	Westerly	10	50	City of Sarnia
3/22/2017	1	17:22-17:41	8	Northerly	-3	52	City of Sarnia
3/23/2017	2	11:10-11:57	15	Southerly	1	42	NOVA Chemicals Industries Facility

736 **Table 2** NO_x/NO_2 ratios for routes driven.

Date	Day's Route Number	Measurement Local Time Period	Number of Points	Average ±1σ	Median
3/21/2017	1	10:26-11:06	37	1.53±0.12	1.49
3/21/2017	2	11:22-11:45	23	1.45±0.06	1.44
3/21/2017	3	12:09-12:28	18	1.36±0.07	1.37
3/21/2017	4	12:34-13:16	24	1.29±0.06	1.31
3/22/2017	1	17:22-17:41	10	1.49±0.53	1.30
3/22/2017	1	17:22-17:41*	9	1.32±0.08	1.30
3/23/2017	1	11:10-11:19	5	1.39±0.09	1.39
3/23/2017	2	11:42-11:57	9	1.46±0.17	1.52

737 The 3/22/2017 17:22-17:41* data had the peak NO_2 plume location NO_x/NO_2 value removed.

738

Table 3 Calculated Leighton Ratios for selected plume maximums on Day 1 and 2.

Date	Local Time	J_{NO2} ($\times 10^{-3}$ s^{-1})	Solar Irradiance (W m^{-2})	Solar Zenith Angle	O_3 mixing ratio (ppb)	Measured NO_2/NO (ppb ppb^{-1})	Calculated Leighton Ratio*
21/03/2017	11:00	5.23	564	35	18	1.7	1.61
21/03/2017	11:30	5.65	600	40	23	2.2	1.76
21/03/2017	12:15	6.44	675	43	23	2.2	2.01
22/03/2017	17:28	2.71	300	23	10	0.5	0.44

*** Note that Leighton ratios,** ϕ , could be biased high by as much as +20% from the the NO_z component of NO_y measured by the NO_x analyzer, but likely much lower due to it being a fresh urban/industrial NO_x plume.

743 **Table 4** Lower limit NO_x Emission Estimates from 10 m elevation wind-speeds.

Date	Emission Source	Daily Route Number	Lower-limit NO_x (tonnes hr^{-1})	NPRI NO_x (tonnes hr^{-1})
21/03/2017	Sarnia	1	1.6±0.8	0.9
21/03/2017	Sarnia	2	1.2±0.5	0.9
21/03/2017	Sarnia	3	1.4±0.5	0.9
22/03/2017	Sarnia	1	1.5±0.6	0.9
22/03/2017	Sarnia	1*	2.2±0.8	0.9
23/03/2017	NovaChem	1	0.27±0.1	0.14
23/03/2017	NovaChem	2	0.29±0.1	0.14

744 * calculated using individual NO_x/NO_2 ratios.

745 **Table 5** Average emission estimates from Mobile MAX_DOAS using 10 m wind-speeds and from NPRI.

	Gas	Lower Limit Emission Estimate (tonnes hr^{-1})	2017 NPRI Value (tonnes hr^{-1})
Sarnia	NO_x	1.60±0.34	0.9
Sarnia	SO_2	1.81±0.83	1.85
NOVA Chemicals-Corunna Site	NO_x	0.28±0.06	0.14

746

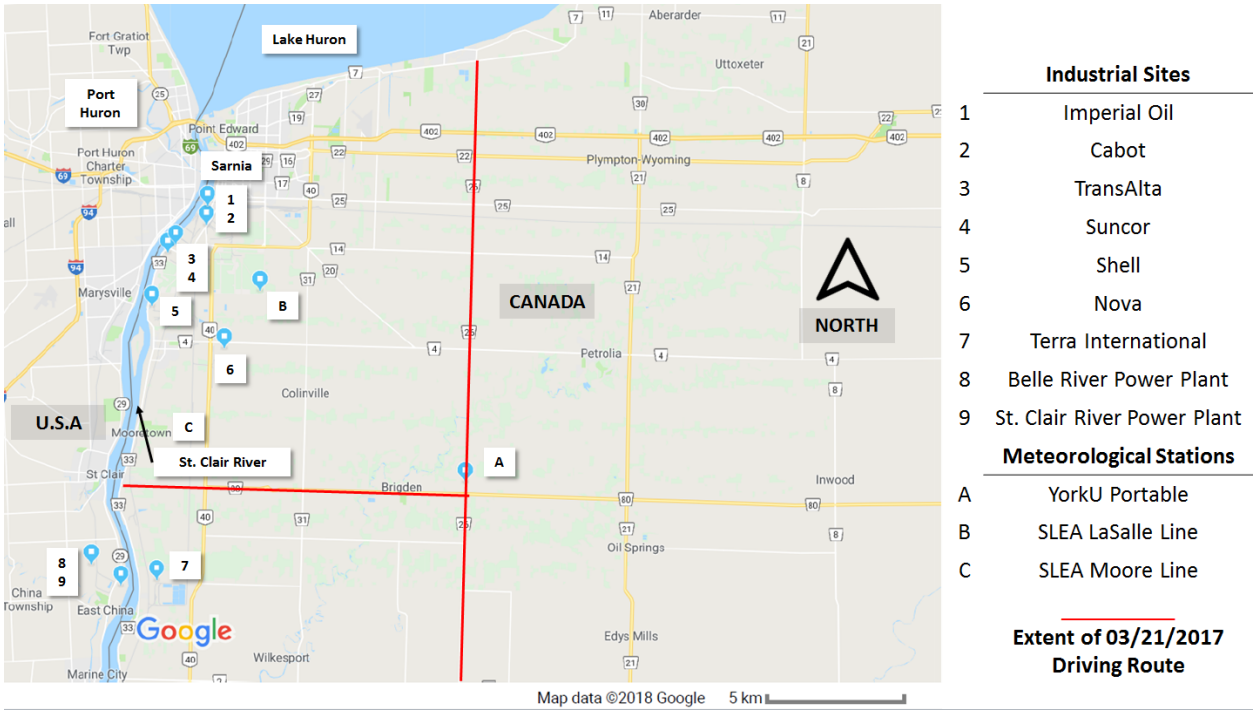

747 **Figure 1** Location of industrial NO_x and SO_2 emission sources and meteorological stations in the Sarnia area.

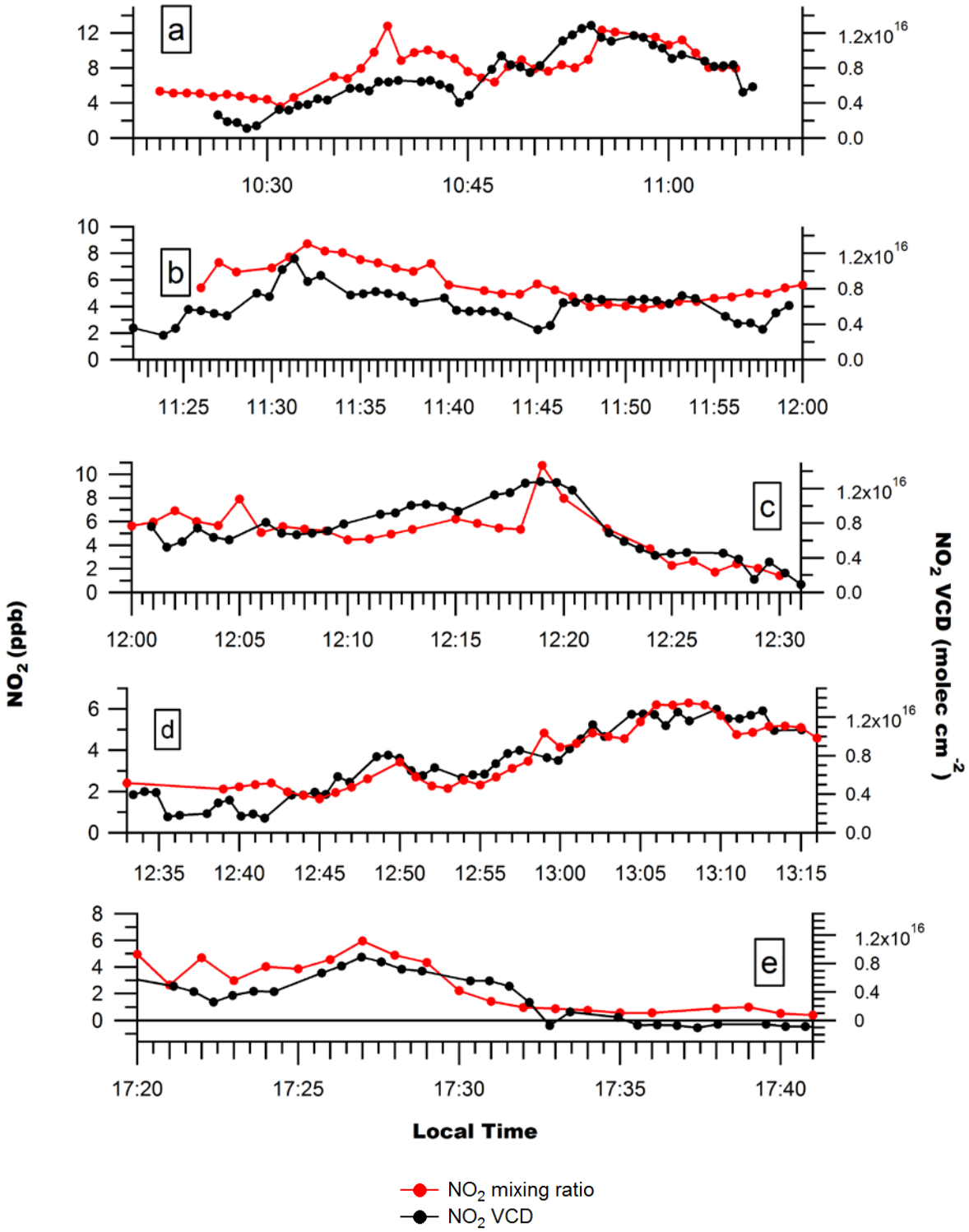

748

749 **Figure 2** NO_2 mixing ratios and NO_2 VCDs along routes 1-4 on Day 1 (a) – (d) and route 1 on Day 2 (e).

750 Uncertainties in measured NO_2 mixing ratios are ± 0.5 ppb. Uncertainties in the NO_2 VCD are given by

751 $\sigma_{VCD} = [(0.25\ VCD)^2 + (5\times10^{14}\ molec\ cm^{-2})^2]^{½}$.

752

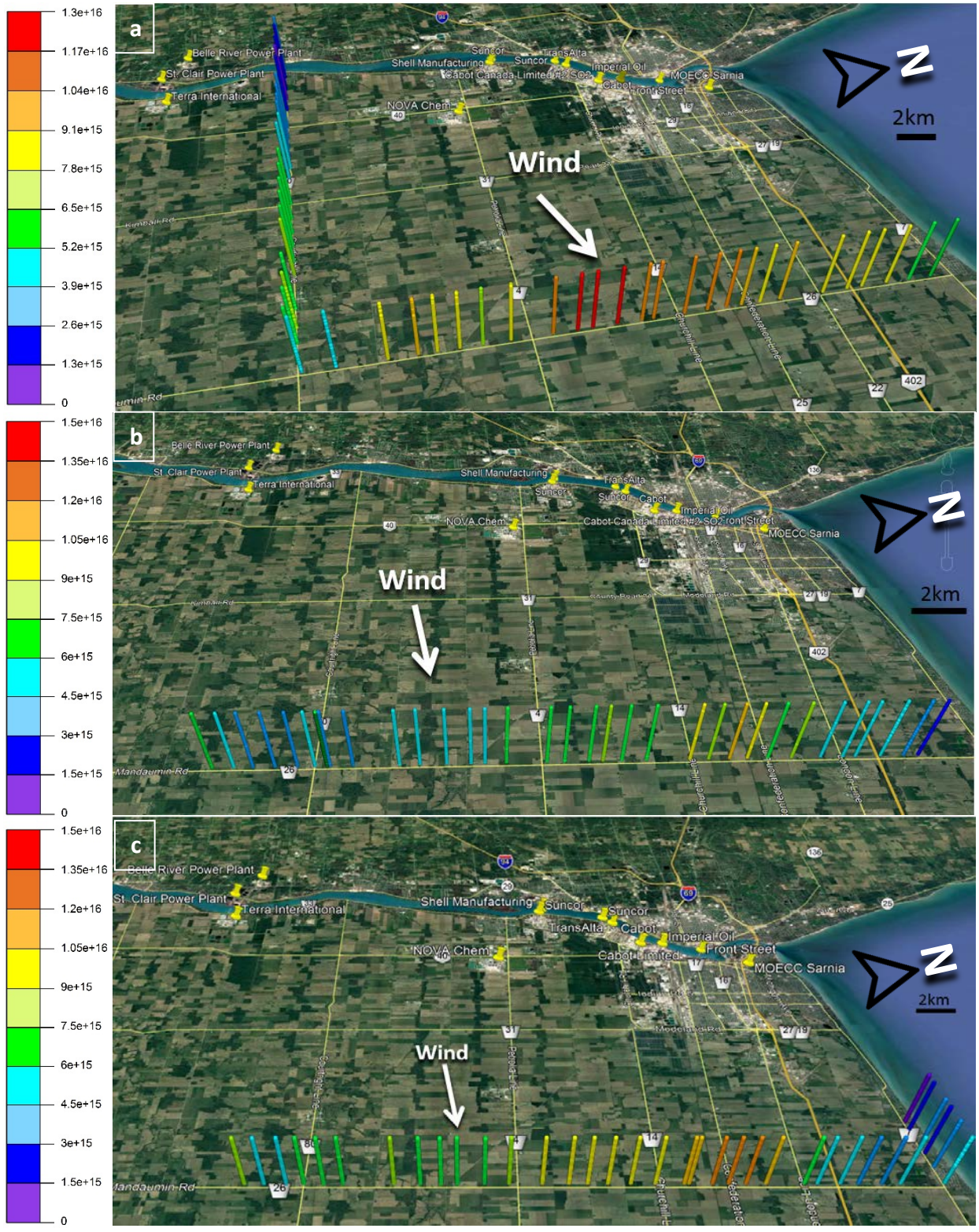

Figure 3 Day 1 driving routes; (a) route 1, (b) route 2 and (c) route 3, used to estimate NO_x emissions from Sarnia.

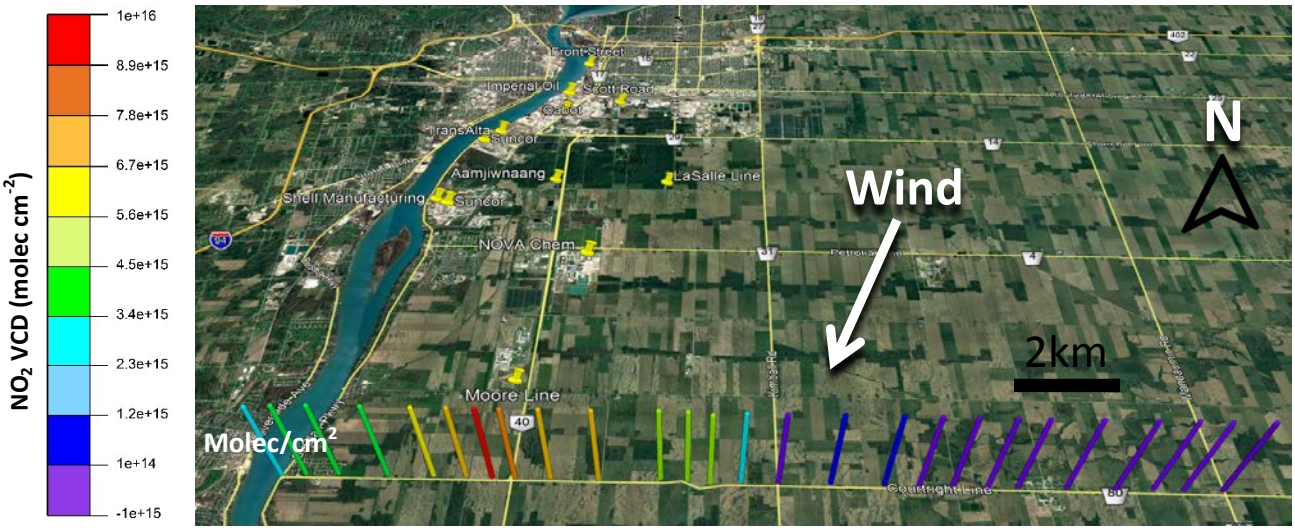

Figure 4 NO_2 VCDs measured on Day 2 route 1.

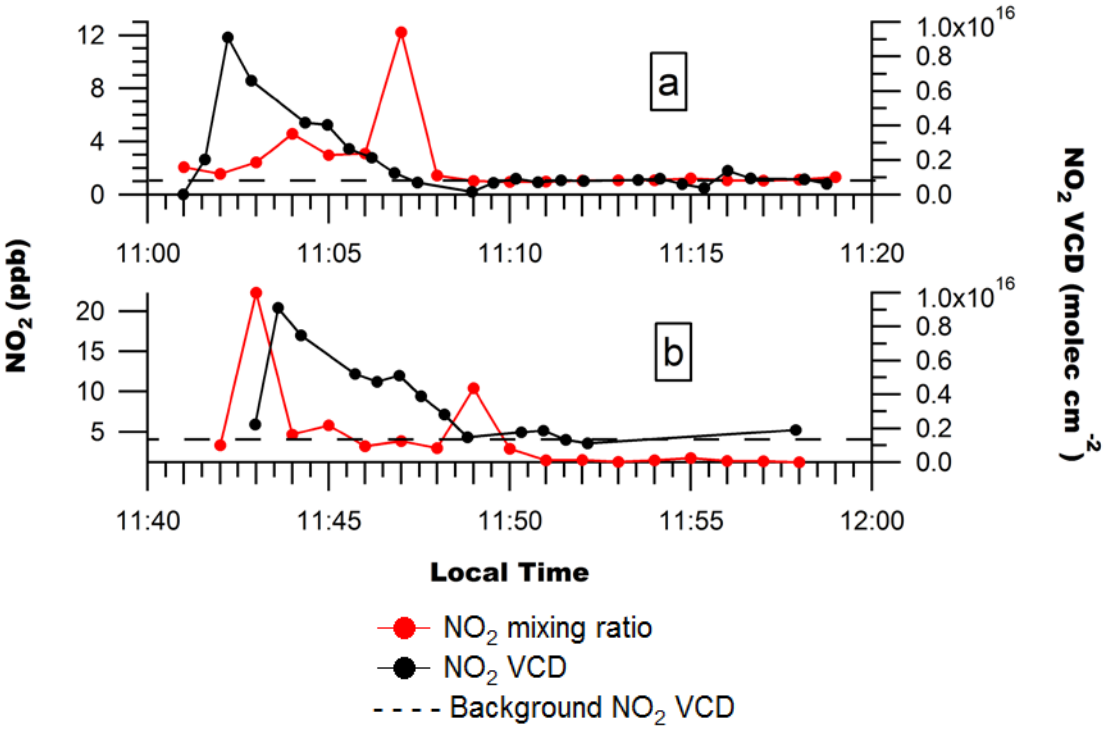

Figure 5 NO_2 mixing ratios and NO_2 VCDs measured on Day 3 along (a) driving route 1 and (b) driving route 2. Uncertainties in measured NO_2 mixing ratios are ± 0.5 ppb. Uncertainties in the NO_2 VCD are given by $\sigma_{VCD} = [(0.25\ VCD)^2 + (5\times10^{14}\ molec\ cm^{-2})^2]^{½}$.

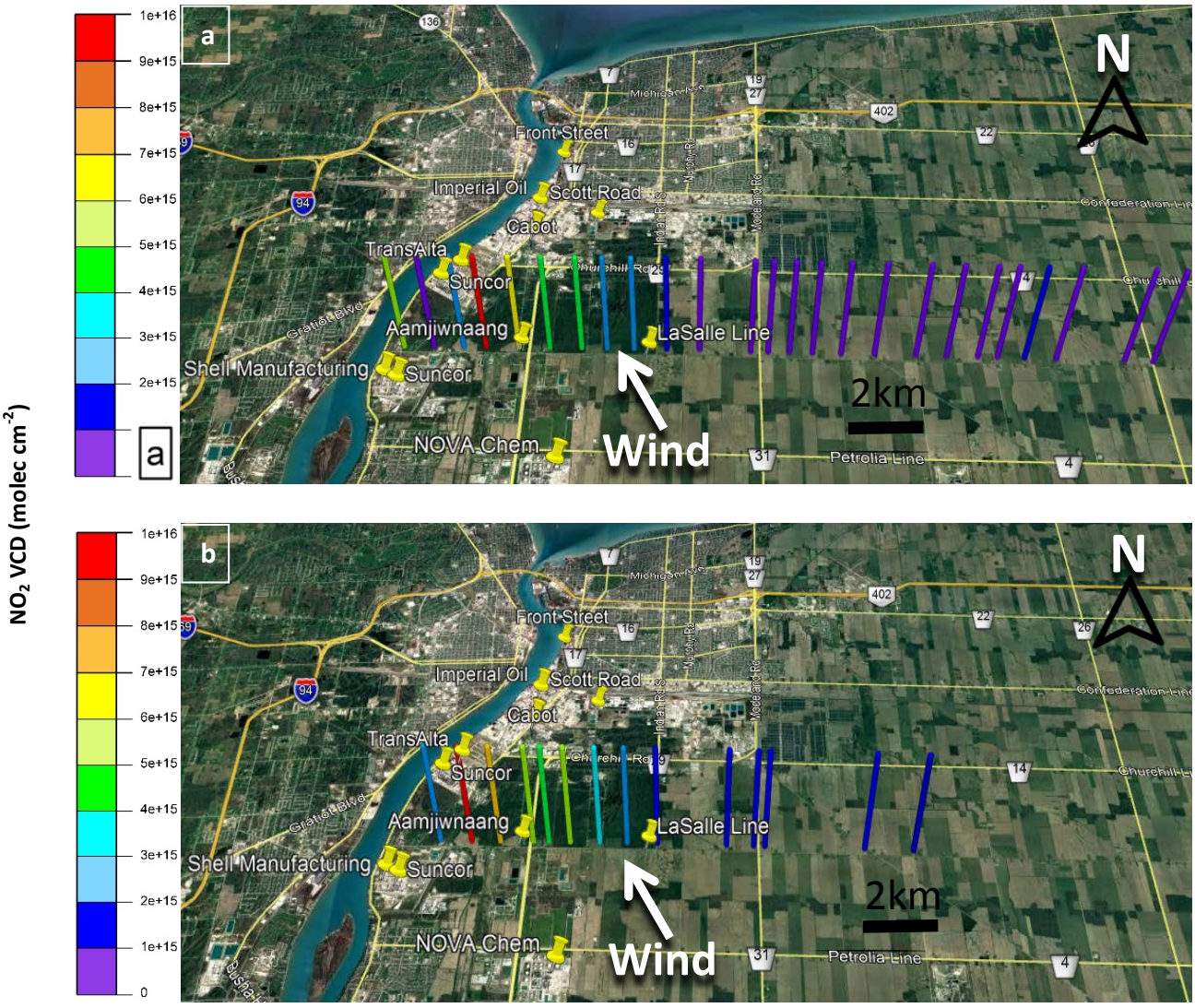

Figure 6 NO_2 VCDs measured on Day 3 along (a) driving route 1 and (b) driving route 2.

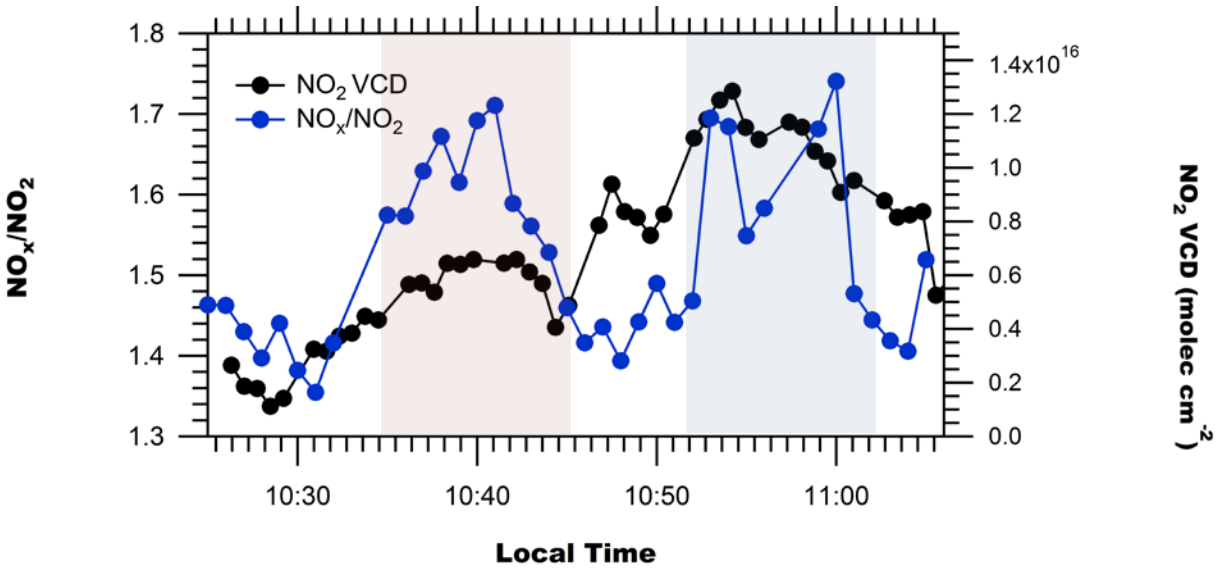

Figure 7 NO_2 VCDs and NO_x/NO_2 ratios on Day 1 route 1. Detection of Michigan power plants' plume(s) (left) on East-West transect & Sarnia plume (right) on North-South transect are highlighted in pink and blue, respectively. Uncertainties in measured NO_x/NO_2 ratios are ± 5% (~±0.075). Uncertainties in the NO_2 VCD are given by $\sigma_{VCD} = [(0.25\ VCD)^2 + (5\times10^{14}\ molec\ cm^{-2})^2]^{½}$.

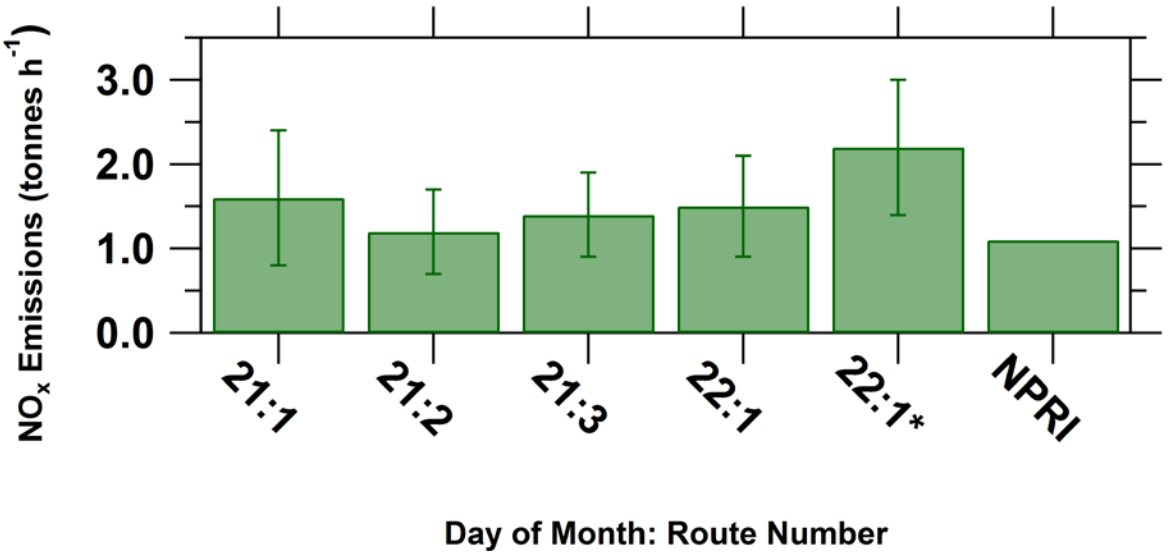

784

785 **Figure 8** Lower limit estimates of NO_x Emissions from Sarnia on Day 1 and Day 3 and 2016 NPRI emissions. The
786 22:1* NO_x emission estimate used individual NO_x/NO_2 ratio values for each VCDs rather than a single average
787 ratio.

788

789

790

791

792 **Figure 9** SO_2 VCDs along route for emission estimate (Day 1 Route 3).

793

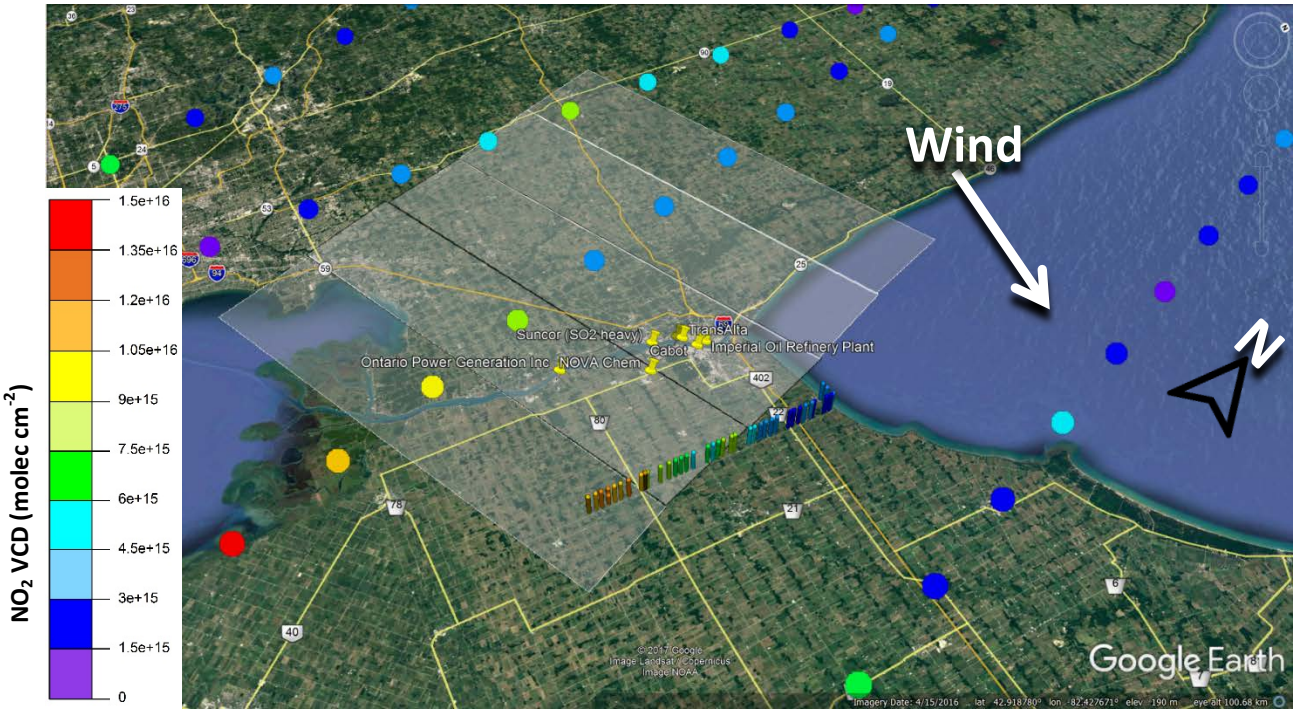

794

795 **Figure 10** Day 1 NO_2 VCDs from OMI satellite VCDs and mobile-MAX-DOAS Route 4. OMI satellite pixels
796 closest to Sarnia were measured at ~18:00 local time. Semi-opaque rectangles centered on the colored dots
797 (indicating satellite VCD value) indicate the spatial extent of the pixel.

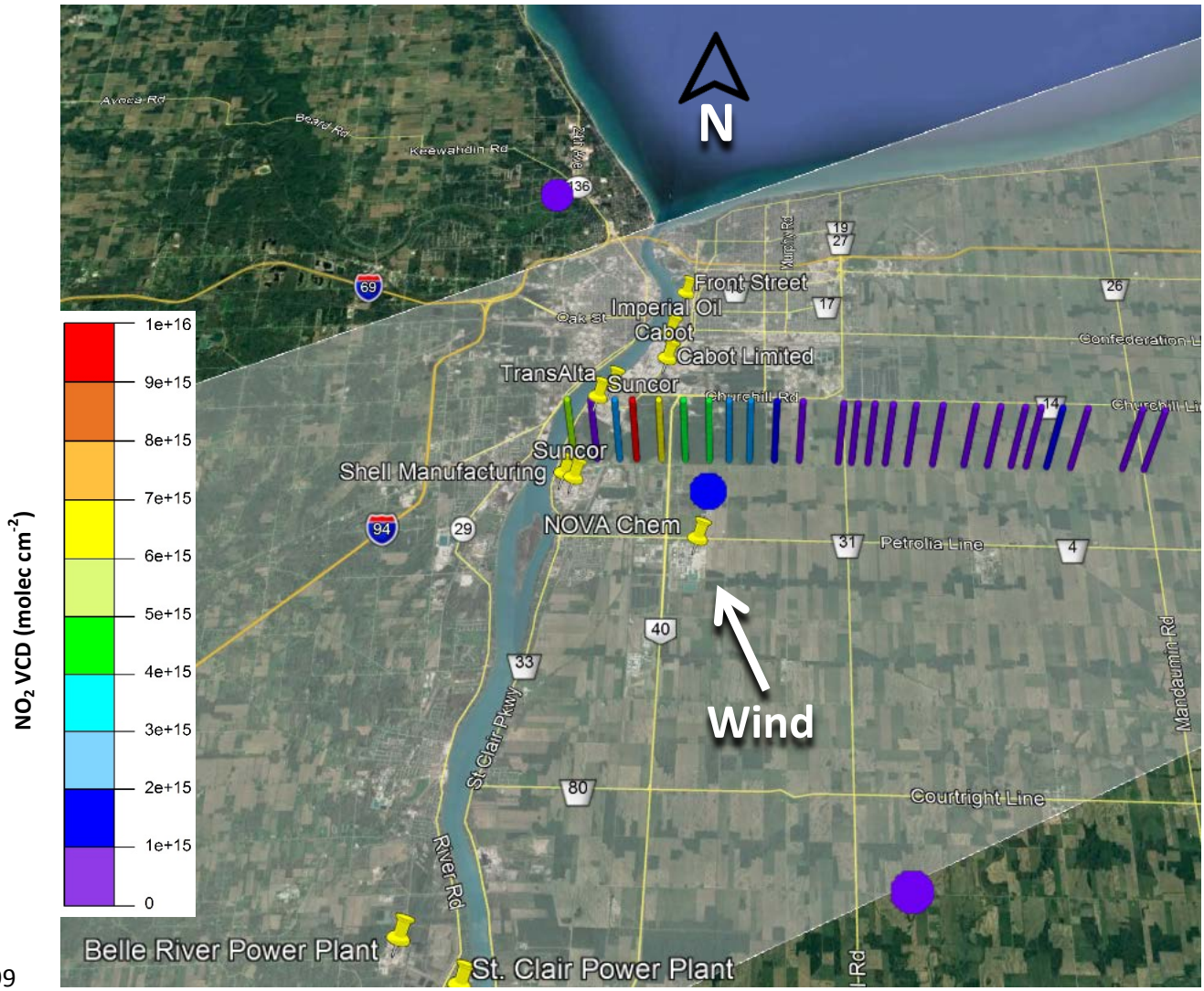

Figure 11 Day 3 NO_2 VCDs from OMI satellite and mobile-MAX-DOAS Route 1. OMI pixels shown were measured at ~18:00 local time. Semi-opaque rectangle centered on the colored dots indicates the spatial extent of the pixel.